



M 2016

# **STEEL REINFORCEMENT FOR TIRES**

## **TEST METHOD DEVELOPMENT TO ASSESS THE ADHESION OF STEEL REINFORCEMENTS TO RUBBER UNDER DYNAMIC CONDITIONS**

**JOÃO PAULO TEIXEIRA DA COSTA**  
DISSERTAÇÃO DE MESTRADO APRESENTADA  
À FACULDADE DE ENGENHARIA DA UNIVERSIDADE DO PORTO EM  
ÁREA CIENTÍFICA

**Mestrado Integrado em Engenharia Química**

***Steel reinforcement for tires- Test Method  
development to assess the adhesion of steel  
reinforcements to rubber under dynamic  
conditions***

**Master's Thesis**

by

**João Paulo Teixeira da Costa**

Developed within the Dissertation Course

performed at

**Continental AG Werk Stöcken**

**Body Compound & Reinforcement Technology Department**



Supervisor at FEUP: Prof. Adélio Mendes

Supervisor at Continental: Dr. Thomas Kramer



Universidade do Porto

Faculdade de Engenharia

**FEUP**

**Departamento de Engenharia Química**

February of 2016



## Acknowledgements

Five months after starting this both professional and personal challenge, I can finish this chapter with nothing else but an enormous pride for all the work I developed. The daily challenges I have faced, the obstacles I have overcome, only made me a better and stronger person. However, I wouldn't be as successful as I was if I didn't have the amazing people I had by my side.

To Dr. Thomas Kramer and Thomas Felten, a special acknowledgement for giving me this outstanding opportunity, all the help provided during this period and all the questions you did not leave unanswered.

To Prof. Adélio Mendes, many thanks for the support and guiding advices which inspired me to succeed in this work.

I also want to express all my gratitude to everyone in the Body Compound & Reinforcement Technology Department for the constant availability and the many good moments provided which turned my integration into an easy task.

A very special thanks to Andreas Maibohm and all the people in the Reinforcement Testing Laboratory, for the many laughs you provided and mainly, even with the language barrier, for trying as hard as you can to help me in any situation.

A special thanks to Alexandre Gomes, Ana Martins, Carla Pires and Diana Pinto of Continental-ITA for arranging me a first contact with the company and some methods which I found very helpful.

A big thank you to Diana Gomes, Miguel Oliveira and Bruno Palma for making me feel at home and for all the availability to help you have always showed during this entire time.

To Gonçalo Ferraz and Marco Iovaldi, two true friendships that I will keep for life, for all the good moments, making my stay in Hannover much more pleasant, a big thank you.

To my three best-friends: Antonino, João e Jorge, for proving me that 2 000 km is only a number and a true friendship always remains no matter in what circumstances, an enormous thank you.

Finally, I have no words to express my gratitude to all my family, especially my parents and brother who mean the world to me, for all the unconditional support you have always given me, for all the patience, willing for guidance and those daily words that made me feel at home. Without you this couldn't certainly be possible.

To all of you, again, Thank You.

---

## Abstract

The main goal for this master thesis is the development of a test method to assess the adhesion performance between steel cord and rubber in tire service conditions, i.e., under dynamic conditions. Ultimately, this test method would be used to compare the real adhesion performance of 3 “experimental compounds” with the adhesion of the reference compound used in commercial vehicle tires (CVT). These 3 new compound recipes were created due to potential use prohibition of resorcinol as well as other hazardous chemicals. To validate the new method the results should match the tire drum-test. Thus, three different tests were designed, all of them involving a mechanical repetitive fatigue and an adhesion assessment steps. The test design would go through several stages, since the sample building, parameter setting appropriate for fatigue and test validation.

The first test developed was the Shear T-Test, a 2-step test, where a modified T-Test sample was placed for a given number of cycles on the Frank Machine. This is a fatigue device that allows either tension fatigue or compression, analyzing the static adhesion at the end of the procedure on other machine, Zwick Tensile Tester. Since there was no hint on which direction to proceed, three research lines were followed to find suitable parameters for the fatigue test (frequency, number of cycles, loading to be applied). An optimized set of loading (tension), frequency and number of cycles was obtained. Concerning the method validation, using modified T-test samples in fresh and humidity-aging conditions, the results did not match with the results obtained with the tire drum-test.

The second test, Dynamic T-test, was a 1-step test method. A standard T-test sample is placed in the MTS device, being fatigued cord by cord, recording the pull-out force along with other variables. The test conditions of the MTS device were 80 °C and 20 Hz. The results of this method matched with the drum-test. Finally, the third test, 3-Cord Adhesion, is still at a preliminary stage of development.

The goal of developing a test method able to assess the adhesion between steel cord and rubber under dynamic conditions was achieved with the Dynamic T-Test, which should be considered for further testing. On the Shear T-Test, better results could have been achieved if the testing procedure allowed the temperature shift.

**Key-words:** dynamic adhesion; steel reinforcement; fatigue; steel-rubber adhesion;

---

## Resumo

O principal objetivo desta tese de mestrado é o desenvolvimento de um método de teste para avaliar a adesão entre cordas de aço e borracha nas condições de serviço do pneu, i.e, em condições dinâmicas. Em última instância, este método de teste será usado para comparar a performance na adesão em 3 “compostos experimentais” com a performance obtida no composto de referência usado em CVT. Estas 3 novas receitas de compostos foram criadas devido à potencial proibição do uso do resorcinol bem como outros químicos nocivos. Para validar o novo método, os resultados do método de teste devem corresponder aos resultados dos testes aos pneus. 3 testes diferentes foram desenvolvidos: em cada um deles, um processo de fadiga mecânica repetitiva seguir-se-ia de um teste de avaliação da adesão. O processo de desenvolvimento do método de teste seria sujeito a várias etapas, desde a construção das amostras, definição de parâmetros apropriados para a fadiga até à validação do método especificado.

O primeiro teste desenvolvido foi o “T-Teste de Corte”, onde uma amostra de T-Teste modificada seria colocada por um dado número de ciclos na máquina de Frank. Este dispositivo permite dois modos de fadiga: tensão e compressão. No final, seria analisada a adesão estática noutro dispositivo, a “Zwick Tensile Tester”. De modo a encontrar parâmetros mais apropriados para o processo de fadiga (frequência, número de ciclos, tipo de carga a ser aplicada), 3 investigações foram levadas a cabo. Um conjunto de parâmetros otimizado foi obtido, definindo o tipo de carga (tensão), a frequência e o número de ciclos. Quanto à validação do método, usando amostras de T-Teste modificadas em condições naturais e de humidade, os resultados não corresponderam aos obtidos nos testes aos pneus.

O segundo teste, “T-Teste Dinâmico”, é um teste de passo único. Uma amostra de T-Teste *padrão* é colocada na MTS, sendo a fadiga efetuada corda por corda, obtendo a força de remoção bem como outras variáveis importantes. As condições de teste da máquina de teste foram 80 °C e 20 Hz. Os resultados deste teste corresponderam aos resultados obtidos nos pneus. O terceiro teste, “Adesão de 3-Cordas”, está numa fase preliminar do seu desenvolvimento.

O objetivo de desenvolver um método de teste capaz de avaliar a adesão entre cordas de aço e borracha foi conseguido através do “T-Teste Dinâmico”, que deve ser considerado para futuros testes. No “T-Teste de Corte”, poderiam ter sido obtidos resultados mais satisfatórios se o procedimento de teste permitisse temperaturas diferentes além da temperatura ambiente.

**Palavras-Chave:** adesão dinâmica; reforços de aço; fadiga; adesão aço-borracha;

---

## Declaration

I declare, under honor commitment, that this work is original and all non-original contributions were properly referred with source identification.

*Sign and date*

# Index

<b>1</b>	<b>Introduction.....</b>	<b>1</b>
1.1	Project Presentation .....	1
1.2	Work goals and contribution .....	2
1.3	Thesis Organization.....	2
<b>2</b>	<b>State of the Art.....</b>	<b>4</b>
2.1	Tires .....	4
2.1.1	Functions .....	5
2.1.2	Composition and structure .....	5
2.2	Reinforcement Materials .....	7
2.3	Rubber Metal Adhesion .....	9
2.3.1	Mechanism of Steel Cord-Rubber Adhesion.....	9
2.3.2	Aging of steel cord-rubber interface .....	11
2.4	Static/Dynamic adhesion .....	11
2.4.1	Tension test methods .....	12
2.4.2	Compression test methods .....	14
<b>3</b>	<b>Test Development Description and Discussion .....</b>	<b>15</b>
3.1	Equipment.....	15
3.1.1	Frank Machine .....	15
3.1.2	Zwick Tensile Tester .....	15
3.1.3	MTS Machine .....	15
3.2	Adhesion Standard tests used/reformed .....	16
3.2.1	Standard Static adhesion T-Test .....	16
3.2.2	Peel Test.....	17
3.3	Tests design and sample preparation .....	17
3.3.1	Shear T-Test .....	17
3.3.2	Dynamic T-Test.....	30
3.3.3	3-Cord Adhesion .....	34



<b>4</b>	<b>Results and Test Method Validation .....</b>	<b>38</b>
4.1	Expected results .....	38
4.2	Test results.....	39
4.2.1	Shear T-Test .....	39
4.2.2	Dynamic T-Test .....	41
<b>5</b>	<b>Conclusions .....</b>	<b>44</b>
<b>6</b>	<b>Project Assessment.....</b>	<b>45</b>
6.1	Achieved goals.....	45
6.2	Limitations and Future Work .....	45
6.3	Final Assessment .....	45
	References .....	46
	Appendix 1- Procedure Dynamic T-Test.....	49
	Appendix 2- Graphs Dynamic T-Test.....	50

# Index of figures

Figure 1-Tire types [4].....	4
Figure 2-Radial tire structure (Adapted from [2] ). .....	6
Figure 3-Steel cord composition ( Adapted from [7]).....	8
Figure 4-Examples for cord constructions. ....	8
Figure 5-Diagram of brass-coated steel cord surface [12]. ....	9
Figure 6- Brass-rubber interface after vulcanization [12]. ....	10
Figure 7-Mechanism of dezincification process in dry and humid conditions [12]. ....	11
Figure 8-Rubber-Steel cord specimen (adapted from [16]). ....	13
Figure 9- Effects of parameters on pull-out-Force:.....	13
Figure 10- a) Frank Machine b) Zwick Tensile Tester c) MTS Machine. ....	16
Figure 11- Standard T-Test Procedure.....	16
Figure 12- Standard T-Test Sample .....	16
Figure 13- Prepared samples a) 4 standard samples in the preparation mould b) Modified T-Test Sample.....	19
Figure 14- Samples placed on Frank Machine. ....	20
Figure 15- Influence of compression/tension in a) Pull-out force b) Coverage. ....	21
Figure 16- Influence of compression/tension in POF on the 2 <sup>nd</sup> investigation. ....	22
Figure 17- Influence of compression/tension in coverage on the 2 <sup>nd</sup> investigation. ....	23
Figure 18-Test deviation evaluation. ....	24
Figure 19-New modified T-test sample setup. ....	25
Figure 20- Influence of compression/tension in pull-out force. ....	26
Figure 21- Influence of compression/tension in coverage. ....	26
Figure 22- Samples in compression.....	27
Figure 23-Results spreading on 3 <sup>rd</sup> investigation. ....	28
Figure 24- 3rd Investigation and re-test results in tension. ....	29
Figure 25- Increase of force level during test.....	30
Figure 26- Relationship between complex, direct and Quadrature dynamic stiffness. ....	31
Figure 27-Phase lag between stress input and strain response [24]. ....	32

Figure 28- $\tan \delta$ curves. ....	33
Figure 29- Pull-out force values. ....	33
Figure 30-a) MTS Machine b) c) Samples set-up for testing. ....	34
Figure 31-a) Curing mould b) schematics of 3-cord sample. ....	35
Figure 32- New 3-cord sample building.....	35
Figure 33- Zwick Machine Set-up for 3-Cord Adhesion Test. ....	36
Figure 34-Mean Peel-Force on Sample 1. ....	37
Figure 35-Mean Peel-Force on Sample 2. ....	37
Figure 36- Tire drum-test results. ....	38
Figure 37- Results Shear T-Test in fresh conditions. ....	40
Figure 38-Results Shear T-Test under humidity aged conditions. ....	40
Figure 39- POF and coverage in Fresh conditions.....	41
Figure 40- Dynamic amplitude displacement in Fresh conditions. ....	42
Figure 41- POF and coverage in humidity aging conditions. ....	43
Figure 42- Dynamic amplitude displacement in humidity aging conditions. ....	43
Figure 43- Complex dynamic stiffness curve in sample 1. ....	50
Figure 44- $\tan \delta$ curve in sample 1. ....	50
Figure 45- Complex dynamic stiffness curve in sample 2 . ....	50
Figure 46- $\tan \delta$ curve in sample 2. ....	50
Figure 47- $\tan \delta$ curve in sample 3 ....	51
Figure 48- Complex dynamic stiffness curve in sample 3 ....	51
Figure 49- $\tan \delta$ curve in sample 4 ....	51
Figure 50- Complex dynamic stiffness curve in sample 4 ....	51
Figure 51- $\tan \delta$ curve in sample 5 ....	51
Figure 52- Complex dynamic stiffness curve in sample 5 ....	51
Figure 53- $\tan \delta$ curve in sample 6 ....	51
Figure 54- Complex dynamic stiffness curve in sample 6 ....	51
Figure 55- $\tan \delta$ curve in sample 7 ....	51
Figure 56- Complex dynamic stiffness curve in sample 7 ....	51
Figure 57- $\tan \delta$ curve in sample 8 ....	51

<i>Figure 58- Complex dynamic stiffness curve in sample 8 .....</i>	<i>51</i>
---	-----------

# Index of tables

<i>Table 1- Parameter setting 1<sup>st</sup> investigation. ....</i>	<i>20</i>
<i>Table 2- 3<sup>rd</sup> Investigation Parameter settings. ....</i>	<i>25</i>
<i>Table 3-Parameters set for Shear T-test.....</i>	<i>29</i>
<i>Table 4- Defined parameters for testing.....</i>	<i>32</i>
<i>Table 5-Defined parameters for Dynamic T-Test. ....</i>	<i>33</i>
<i>Table 6-Parameters setting for 3-Cord adhesion. ....</i>	<i>36</i>
<i>Table 7-Sample Notation.....</i>	<i>39</i>
<i>Table 8- <math>\tan \delta</math> and <math>K^*</math> values in fresh conditions. ....</i>	<i>41</i>
<i>Table 9- <math>\tan \delta</math> and <math>K^*</math> values in humidity aged conditions .....</i>	<i>42</i>

# Notation and Glossary

## *List of variables*

$A$	Amplitude	mm
$d$	Dynamic displacement amplitude	mm
$F$	Force/Load	N
$f$	Frequency	Hz
$K^*$	Complex Dynamic Stiffness	N/mm
$\tan \delta$	tangent $\delta$ / loss tangent	dimensionless
$T$	Temperature	°C

## *List of acronyms*

AG	Aktiengesellschaft
CVT	Commercial Vehicle Tires
EU	European Union
POF	Pull-Out Force
RT	Room Temperature

# 1 Introduction

## 1.1 Project Presentation

The present research took place at the Body Compound & Reinforcement technology department of Continental AG. Continental was founded in Hanover in 1871 as the stock corporation “Continental-Caoutchouc- und Gutta-Percha Compagnie”. The manufacturing at the main factory in Hanover included soft rubber products, rubberized fabrics, and solid tires for carriages and bicycles. It evolved greatly since then and today, Continental ranks among the top 5 automotive suppliers worldwide [1].

Nowadays, Continental Corporation is divided into the Automotive Group and the Rubber Group, and consists of five divisions: *Chassis&Safety*, *Powertrain*, *Interior*, *ContiTech* and finally the main division which will be in focus on this thesis, the *Tires* division [1].

As a complex technical component of today’s vehicles, the tire must perform a wide range of functions as cushioning, dampening, assuring good directional stability, and providing long-term service. Summarizing, it must be able to assure ideal and reliable road holding quality, doing all this even when the road provides little traction in wet or slippery conditions or when the road is covered with snow or ice [2].

To satisfy all these contradictory requirements, steel cord has drawn attention and gained popularity as a reinforcement material, especially as a carcass and belt material. Being a composite structure, durability of tire mainly depends on the integrity of the bond between elastomer and the reinforcing cords, i.e., rubber and steel cord [3].

Thus, strong adhesion strength and a meaningful method to test the adhesion strength are primary prerequisites for the development of a durable tire.

Over the years, several tests to assess the adhesion were developed, most of them static by nature. Although these tests are helpful in detecting obvious deficiencies of rubber bonding, they are not sensitive to subtle changes and do not reflect or simulate the service condition of the tire [3]. Therefore, the development of a dynamic test sensitive to these changes is extremely important and more meaningful as far as the prediction of the tire durability is concerned. This was the purpose of this master’s thesis: reproduce this changes sensibility in a way that current tests are not able to.

## 1.2 Work goals and contribution

The development of a test method that indicates the real adhesion performance of steel cord to rubber arises as even more urgent due to potential prohibition of resorcinol as well as other hazardous potential chemicals in the focus of the EU (Cobalt, Formaldehyde). This will require the quick development of new compounds with reduced incorporation of resorcinol. On the other hand, the long term approach looks forward to the development of a whole new adhesive technology.

At the moment, performance of tires made using the new recipes can only be assessed at a plant using drum-tests. This approach leads, however, to considerable high costs and waste of time. The objective of this project is then to elaborate a laboratory scale test that allows testing these new different compounds at lab scale, achieving results matching with the tire tests. Within the scope of this thesis, 4 different compounds were assessed (Reference + 3 experimental compounds).

## 1.3 Thesis Organization

This thesis is organized in 6 chapters, being each of them outlined on the next paragraphs:

**Chapter 1, Introduction-** gives some information about Continental and its organization, introducing as well the main goals and contributions of this thesis;

**Chapter 2, State of the Art-** a deeper introduction to tires technology along with an introduction to reinforcement materials, a section concerning the rubber-metal adhesion and a contextualization into the thematic of dynamic adhesion;

**Chapter 3, Test Development Description and Discussion-** Explains the methodology and technology used during this project, describing and discussing the different test methods. This is the most important part of the thesis: the task execution;

**Chapter 4, Results and Test Method Validation** - refers all the results obtained with the tests developed. Then, a comparison with the real tire tests in order to validate the methods is done;

**Chapter 5, Conclusions** - summarizes the main conclusions taken throughout the research;

**Chapter 6, Project Assessment** - gives an idea of how successful this thesis was, pointing out the goals achieved, describing all the pending subjects and further studies that can be done;



## 2 State of the Art

In this section, all the theoretical background needed for this thesis is presented. An introduction to the tire field, comprising its evolution along the years, its functions and composition is given. The reinforcement materials, especially the steel cord reinforcements, are also addressed. To understand the adhesion phenomena, a brief literature survey on rubber-metal adhesion is presented. Finally, the static/dynamic adhesion characterization is introduced and explained thoroughly.

### 2.1 Tires

As the only contact with the road, the relevance of the tires in a vehicle is rather obvious, whether referring to a simple bicycle or to a more complex vehicle like a car. To most of the consumers, tires are seen as low-tech commodity, making purchasing decisions solely based on price. However, it may be surprising for them to find out that the tire comprises 20 or more components as well as a massive amount of machinery and processing involved in order to achieve the finished product [4].

It is a commodity in constant evolution, which has evolved from the simple wheel 5,000 years ago to the pneumatic tires in the late 1800s as an upgrade from solid rubber tires. These ones had small cross-sections and high pressures, mainly for bicycle applications. In the early 1920's, larger “balloon” tires were introduced with applications in the mushrooming motor vehicle industry. Later, tubeless tires were introduced with improvements in rim design [1].

Nowadays, two types of pneumatic rubber tires dominate the tire market: bias and radial ply.

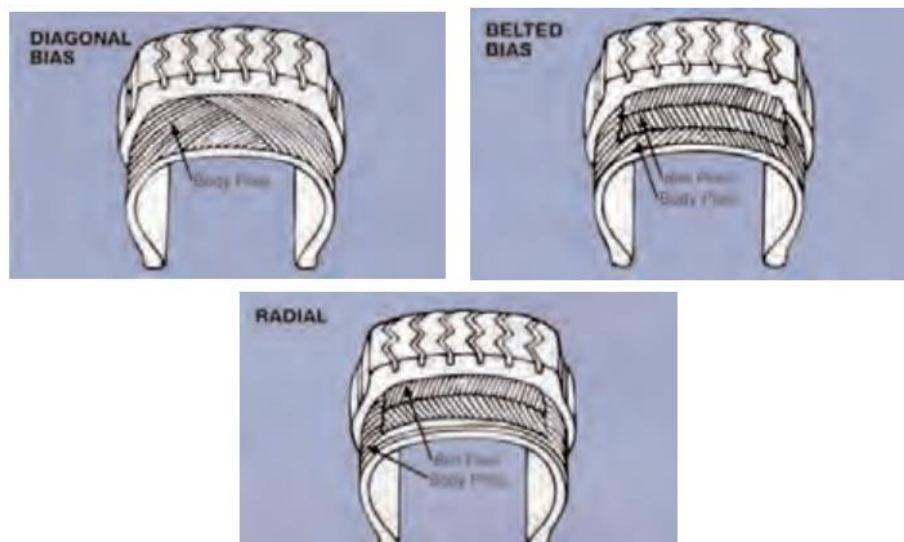


*Figure 1-Tire types [4].*

Regarding the bias tires, they are characterized for having body ply cords laid at angles substantially less than  $90^\circ$  to the tread centerline, extending from bead to bead. On the other hand, radial tires have body ply cords laid radially from bead to bead, nominally at  $90^\circ$  to the centerline of the tread, having two or more belts laid diagonally to add strength and stability, as shown in *Figure 1*. Although the choice of whether using bias or radial tires strongly depends on the country, radial tires still remain as the market dominants.

### **2.1.1 Functions**

Tires must be capable to provide a wide range of functions:

- Vehicle to road interface, where the small patches of rubber are expected to guide us safely in a rainy storm or to allow us to turn fast at an exit ramp or to negotiate potholes without damage;
- Support vehicle load, where the balancing of the tires' internal air pressure can prevent the tire deflect;
- Road surface friction, resulting the ability of the vehicles to start, stop and turn corners;
- Absorb road irregularities, acting as a spring and damper system to absorb impacts and road surface irregularities under a wide variety of operating conditions [4];

Summarizing, the tire must cushion, dampen, assure good directional stability and provide long-term service [2].

### **2.1.2 Composition and structure**

Modern day's tires contain diverse ingredients in different amounts, varying according to the tire size or type (summer or winter tire).

In a succinct way, the tire main components are rubber (natural and synthetic), fillers (carbon black, silica...), reinforcing materials such as steel, polyester, rayon or nylon, plasticizers, chemicals for vulcanization and anti-aging agents or other chemicals [2].

All these materials result in a complex and highly engineered structure which is the tire, whose main sections are illustrated in *Figure 2*:

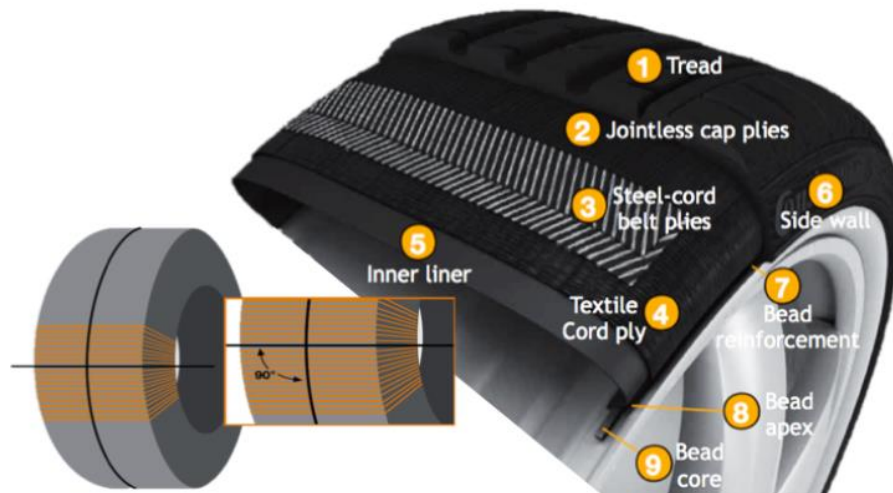


*Figure 2-Radial tire structure (Adapted from [2] ).*

By the numerical order shown on the *Figure 2*, it is explained the tire components and its functions [2]:

**1-Tread:** Made of synthetic and natural rubber, it should promote good road grip and enable water expulsion;

**2- Jointless cap-ply:** Constituted by nylon embedded in rubber, its primary function is the enhancing of high-speed suitability;

**3- Steel-cord belt plies:** Its main function is the optimization of direction stability and rolling distance;

**4-Carcass ply:** Having as materials rayon or polyester rubberized, it should control the internal pressure and maintain the tire's shape;

**5-Inner liner:** Composed by butyl rubber, its low air permeability ensures the air pressure inside the tire;

**6-Side wall:** flexible structure composed by rubber, protecting the casing from external damage and atmospheric conditions;

**7-Bead Reinforcement:** Layers of textile reinforcements, promoting directional stability, steering and performance;

**8- Bead apex:** Composed by synthetic rubber, it should increase the stiffness in the sidewall and bead area, enhancing directional stability, steering precision and improving comfort;

**9- Bead core:** Made of steel wire embedded in rubber, it is used to ensure that the tire is firmly sits on the rim;

## 2.2 Reinforcement Materials

Reinforcing systems play an important role on the tire field since many elastomer types are too weak to be used without some reinforcing system [5].

These reinforcing systems or reinforcement materials are the predominant load carrying members of the cord-rubber composite, providing strength and stability to the sidewall and tread as well as maintain the air pressure.

There are different types of reinforcement materials, each with a different usage and function, listed below [4]:

**Nylon**, a tradename for aliphatic polyamides (PA66), has its main application in medium/heavy truck tires and off-road equipment.

**Polyester** is the condensation polymerization product of ethylene glycol and terephthalic acid, mainly used in radial body plies with some limited applications as belt plies. Its low cost combined with high strength with low shrinkage and low service growth makes it a good choice for passenger and small light truck tires.

**Rayon** is a body ply cord or belt reinforcement made from cellulose. In spite of its stable dimensions, heat resistance and good handling characteristics, the price and the environmental manufacturing issues in the production facilities are not so appealing.

**Aramid**, a synthetic and high tenacity organic fiber, is two to three times stronger than polyester and nylon. His relatively high cost combined with processing constraints has slowed its application as a belt or stabilizer ply material.

**Steel cord** is carbon steel wire coated with brass that has been drawn, plated, twisted and wound into multiple-filament bundles. It is the main belt ply material used in radial passenger tires.

This research focused completely on steel cord reinforcements.

### Steel cord reinforcements

Steel is a metal alloy which major component is iron, with carbon content between 0.02% and 1.7% by weight. Carbon and other elements act as a hardening agent, preventing dislocations in the iron atom crystal lattice from sliding past another. Nowadays, several classes of steels replace carbon with other alloying materials given the fact that carbon, if present, is undesired [5].

The excellent heat and fatigue resistance with no contraction, the fact of being stronger than fiber materials makes steel cord one of the major components used for

reinforcing a radial tire. Its composition is characterized by the presence of four basic components that can easily be seen in *Figure 3* and described below [6]:

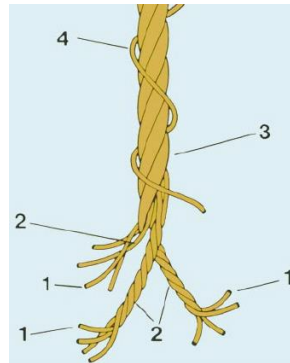


*Figure 3-Steel cord composition ( Adapted from [7]).*

- 1- **Filament or wire**, which is a metal fiber used as individual element in a strand or cord;
- 2- **Strand**, a group of steel filaments twisted together. Several strands may be twisted to form a cord or cable;
- 3- **Cord**, a structure composed by two or more filaments when used as an end product or a combination of strands or filaments and strands;
- 4- **Spiral Wrap**, a filament wound around a steel cord to keep the large cord structure together;

Regarding the cord construction naming rules, usually each construction is described by the formula:  $N \times F \times D + N \times F \times D + N \times F \times D + \dots$ , where  $N$  is the number of strands,  $F$  the number of filaments and  $D$  represents the filament diameter. In *Figure 4* there are some examples of cord constructions:

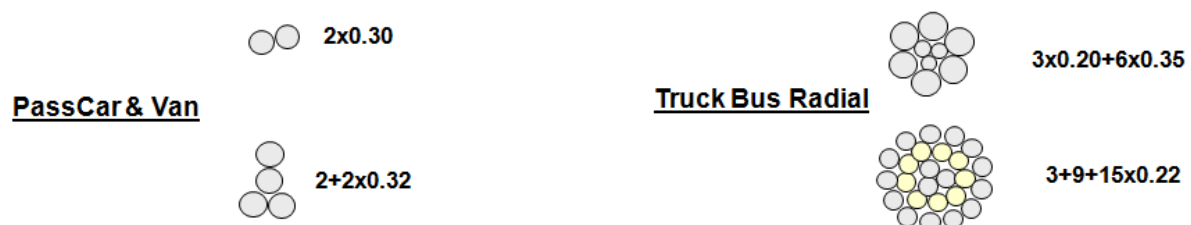


*Figure 4-Examples for cord constructions [7].*

The usage of steel cord in tires depends greatly on the type of tire to be built. In passenger car tires, steel cord is used in the belt while in truck radial tires steel cord is used both in the belt and in the carcass [8].

In the belt it is supposed that the steel cord provides directional stability and performance increasing by its influence on the stiffness of the belt package. On the other hand, in the carcass, specifically in the bead core, steel cord should ensure that the tire sits firmly on the rim.

## 2.3 Rubber Metal Adhesion

Rubber to steel adhesion is of considerable practical importance in the present-day application of steel cords as a reinforcement material in radial tires. It is a standard procedure that steel cords incorporated in tires are brass coated to provide a proper adhesion between rubber and metal given that steel itself is not able to bind to rubber.

This rubber-brass bond is durable and resistant to high temperatures as well as dynamic loading.

### 2.3.1 Mechanism of Steel Cord-Rubber Adhesion

Brass layers usually consist of 60 % - 70% copper [9]. When the brass coated-wire is drawn during the forming process, zinc ions diffuse to the surface where they are oxidized. The enriched zinc oxide layer passivates the brass surface, which contains metallic copper and is covered by a very thin copper oxide film [10, 11]. In *Figure 5* is shown a diagram of brass-coated steel cord surface.

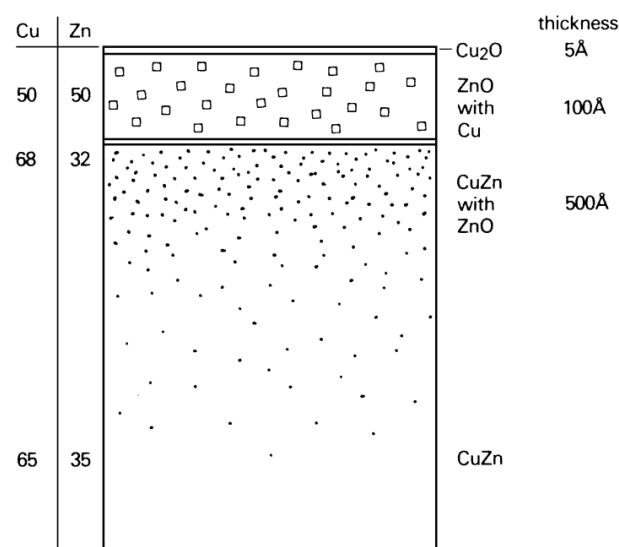


*Figure 5-Diagram of brass-coated steel cord surface [12].*

Contextualizing, vulcanization is the process where rubber is mixed with a combination of additives called vulcanization system and heated in a mold under pressure [10]. The sulfidation reaction occurs at the beginning of this process, allowing the electrons and zinc ions migration to the brass surface before the completion of the rubber crosslinking. Note that metal oxide and sulfide structures are imperfect. These defect points are the permit for diffusion processes [10].

During the vulcanization, exposure of the brass surface to active sulfur creates a strong bond by the action of an interfacial layer which grows before the rubber is crosslinked. At an early stage of vulcanization, copper ions, zinc ions and free electrons move to the brass wire surface and a copper sulfide layer is formed. Zinc sulfide forms initially but at a later stage it is overgrown by copper sulfide. Later, copper ions incorporated in the zinc oxide layer migrate to the top of zinc sulfide surface, building dendritic  $\text{Cu}_x\text{S}$ . In these first stages of sulfidation, zinc forms slowly due to the fact that copper ions have a larger radius than zinc ions. Thus, their migration through the zinc lattice is sterically hindered. On the other hand, there is acceleration in copper diffusion [12].

The copper sulfide layer keeps growing, leading to more  $\text{Cu}_x\text{S}$  dendrites. There is an optimum thickness for the  $\text{Cu}_x\text{S}$  layer that imparts maximum adhesion, if the layer becomes too thick, adhesion is reduced because the copper sulfide dendrites changes from an amorphous into a more crystalline and brittle form.

According to van Ooij, the complete growth of the  $\text{Cu}_x\text{S}$  layer before crosslinking begins is one of the key factors for adhesion capabilities maintenance. In *Figure 6*, a typical rubber brass interface after vulcanization is shown.

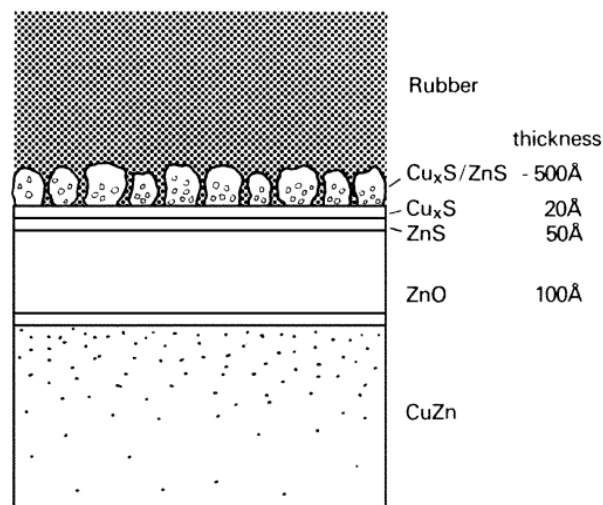


*Figure 6- Brass-rubber interface after vulcanization [12].*

### 2.3.2 Aging of steel cord-rubber interface

Several processes may lead to rubber-brass bond degradation, like thermal aging or electrochemical corrosion [10]. When the copper sulfide stops growing, zinc ions diffuse to the interfacial layer to create more zinc oxide. The zinc ion diffusion can be a slow process under dry conditions but with the eventual development of zinc oxide at the metal surface, the bond is consequently weakened. In humid conditions, the process is accelerated by altering the rate of diffusion of the zinc ions, decreasing the adhesion strength. This consumption is called dezincification and considered as the cause of adhesion failure [12]. The mechanism of the dezincification process is shown in *Figure 7*:

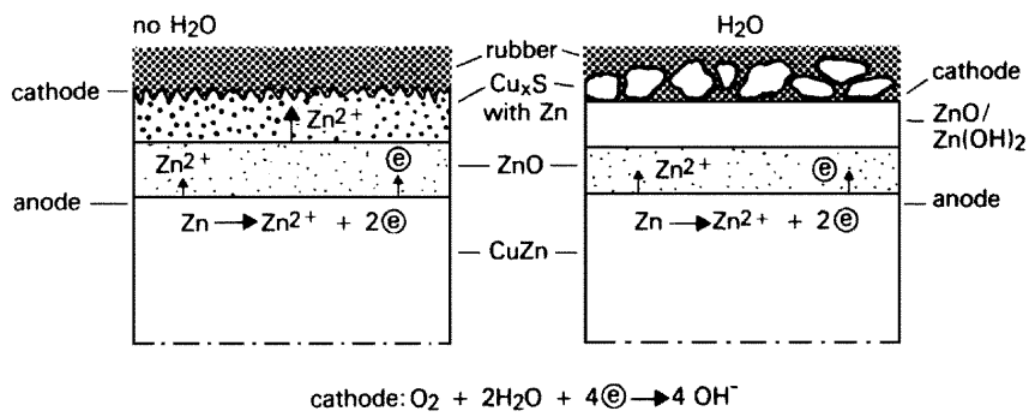


*Figure 7-Mechanism of dezincification process in dry and humid conditions [12].*

### 2.4 Static/Dynamic adhesion

The adhesion strength evaluation has been gaining an increasing interest over the years, originating the development of a considerable number of tests. These tests are basically either static or dynamic in nature [13]. In the tire industry, most of the methods used are static, such as:

- H-adhesion;
- Standard T-Test;
- 90/180° Peel Test;
- Tire Cord Adhesion Test;
- Co-Axial Shear Pull-Out Test;

However, the constant doubt concerning the results obtained in the laboratory are or not an indication of the real adhesion properties of a product is a serious problem. These static adhesion assessment tests are widely used but their validity for dynamic testing is being questioned [14].



The first dynamic adhesion testing technique was introduced in 1940. With the rapid growth of radial tires, much more interest in dynamic adhesion testing came up and several rubber to cord adhesion assessment tests were developed. Most of them can be classified in two different categories on the basis of the mode of deformation, e.g., tension and compression.

#### **2.4.1 Tension test methods**

Two types of test methods can be described as tension test methods. In the first one, either the rubber is fixed or the cord or the metal plate is tensioned directly. In either case, it is not easy to deform the cord and the rubber moves easily. So, a repeated strain is applied to the cord rubber boundary surface, causing fatigue deterioration [15]. This type of test methods is the most typical method of evaluation of all dynamic adhesion tests. The most popular dynamic test techniques are [3]:

- Buist method;
- Ivenger method;
- Voracheck method;
- Khromove method;
- Wagner disc-fatigue method;

Many more tests could be mentioned but a recent research developed by a group of researchers in China will be in focus for this thesis. This novel testing technique for the adhesion of rubber compounds was developed to focus on simulating the cyclic loading of carcass in real service. The purpose was the investigation of the effects of fatigue frequency, temperature and number of cycles on the adhesion rubber to steel cord as a possible way to predict the adhesion life of tires.

The rubber/steel cord specimen is developed accordingly to how they were adhered in a carcass, as shown in *Figure 8* [16]. Previous studies indicated that the adhesive strength between rubber and steel cord degraded much faster during aging. Other studies reflected that the ambient temperature carried out during testing is crucial [14]. The specimens were subjected to a repetitive flex fatigue with tension deformations of 4 mm of the rubber bars at the selected temperature, frequency and number of cycles.



Figure 8-Rubber-Steel cord specimen (adapted from [16]).

After a given number of fatigue cycles, the steel cords between the two rubber bars were immediately cut into two equal lengths. After a 32 h sample storing, the T-pull-out forces were measured using a Zwick tensile tester, where the average of the two “pull-out force” measurements was considered as the result. The results of the effects on the three different parameters are shown in Figure 9 a), b) and c):

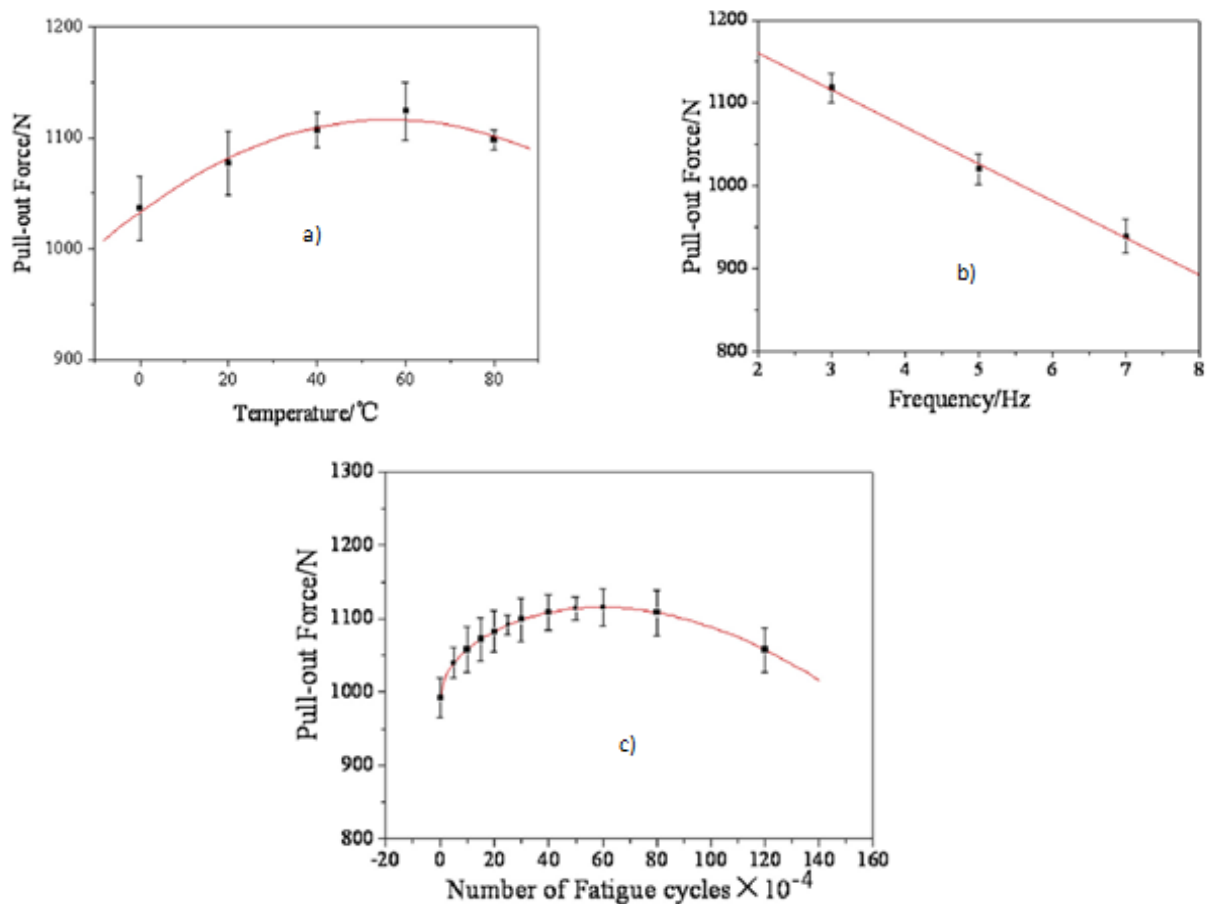


Figure 9- Effects of parameters on pull-out-Force:

a) Temperature b) Frequency c) Number of cycles (adapted from [16]).

By observation, it is given that the dynamic “pull-out forces” decreased with an increase in fatigue frequency. About the temperature influence, the dynamic “pull-out forces” first increased and then decreased with increasing temperature with a maximum at approximately 60 °C.

Finally, the dynamic pull-out forces did not change significantly as the number of fatigue cycles increased from 0 to 1 200 000 although again a maximum can be interpreted at approximately 600 000 cycles. The pull-out force after fatigue was invariably greater than before fatigue although the tendency shown may be an indicator that if increasing even more the number of fatigue cycles, the pull-out force may reach a minimum being an indicator of an impact in the adhesion layer.

#### **2.4.2 Compression test methods**

Two types of compressive adhesion fatigue tests can be described. The first type is a falling weight repetitive impact type test while the other one involves the use of a flexometer in which a compressive deformation of fixed amplitude is applied under a constant load. Both methods use well known equipment and are supposed to be effective for the simulation of adhesion fatigue phenomena [17].

##### *Impact type test methods*

The Dunlop Fatigue Tester was first described in 1941, where with this machine the repetition rate onto the rubber block which forms the sample is 150-300 times per min. Also, with this tester, fixed load, fixed displacement and fixed energy tests can be carried out. Most of the methods involve testing machines similar to Dunlop Fatigue Tester but with the incorporation of various improvements.

##### *Flexo-type test methods*

This method involves embedding a cord in a sample and assessing the adhesion fatigue degradation after repeated compression using a flexometer or similar device. The features of this test are that adhesion fatigue degradation is produced at the cord-rubber bonding surface by a shear strain that results from the compression, simulating the situation in a running tire [17].

## 3 Test Development Description and Discussion

This chapter explains the methodology and technology used during this project. Three different dynamic tests are described and discussed: from the parameter setting, materials and machinery used to the procedure followed to carry out the sample building and tests.

### 3.1 Equipment

Different machinery was used according to the specifications and methods of the test procedures. Below the main equipment used is enunciated:

#### 3.1.1 Frank Machine

This apparatus, as shown in *Figure 10 a)*, is designed as a simple mechanical fatigue device, testing molded samples by a repeated motion. The bottom bar is the only machine piece in motion. If the desired loading to be applied is tension, the samples should be placed when the bar hits its highest point. If, on the other hand, the point is to compress the samples, they should be placed in the lowest point of the bar. It includes a cycle counter fitted with 99 999 999 cycles allowed per test, with a frequency range of 0 Hz - 10 Hz and maximum amplitude of around 25 mm. Despite being very useful, the fact of not having a temperature chamber constitutes a serious disadvantage, allowing only the fatigue at room temperature.

#### 3.1.2 Zwick Tensile Tester

Zwick Tester, see *Figure 10 b)*, is suitable for applications in all fields. It is available with test speeds from 0, 00005 to 3000 mm/min, test loads up to 250 kN and test-area heights from 1030 mm to 2560 mm [18]. Operating through a computer software, it allowed the adhesion assessment by static pull-out tests of several samples as well as a 'modified Peel-test'.

#### 3.1.3 MTS Machine

The MTS machine, see *Figure 10 c)*, is a high force servohydraulic test system, offering a wide range of test applications, from a simple, static characterization to complex, dynamic life studies. A servo hydraulic system consists of a control system that measures the output, forcing it to follow a command signal. This machine allows a point-by-point monitoring, giving the user the opportunity to perform calculations and making decisions on every data point rather than making decisions once per test [19].

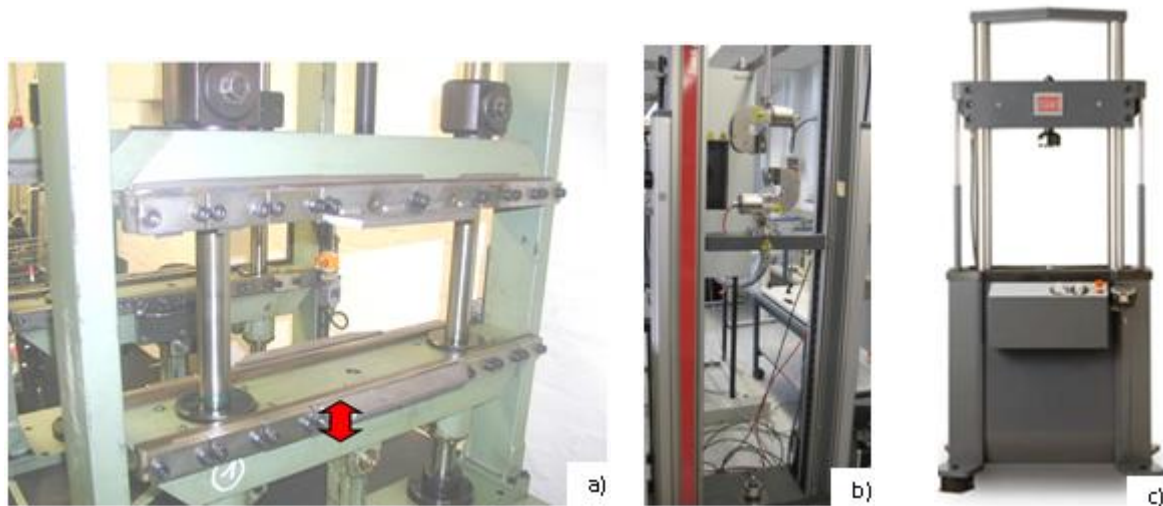


Figure 10- a) Frank Machine b) Zwick Tensile Tester c) MTS Machine.

### 3.2 Adhesion Standard tests used/reformed

All the tests described below were either used originally or reformed according to the needs of the test developed.

#### 3.2.1 Standard Static adhesion T-Test

This test measures the force necessary to pull out the cord thread from a test specimen with defined dimensions. The test is carried out in the Zwick or MTS machine and its specimen is similar to the one shown in *Figure 11*. An example of the procedure followed is represented in *Figure 12*. The specimen is clamped in the Zwick Tensile Tester, the cords are pulled till the moment the cords detach the rubber matrix, obtaining the information of the “pull-out force”.

Another parameter evaluated is the rubber coverage. Evaluated by the operator, it is measured on a scale from 65 % to 100 %, with a step unit of 5 %. The lower value represents the total absence of rubber coverage, with bare cords visible while the highest value represent a fully rubber covered specimen.

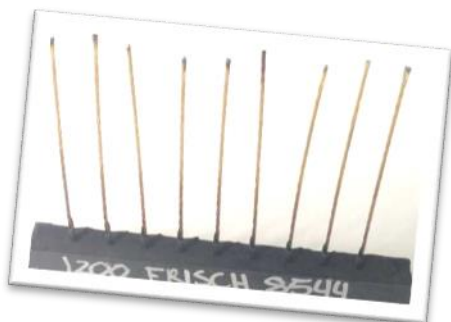


Figure 11- Standard T-Test Sample

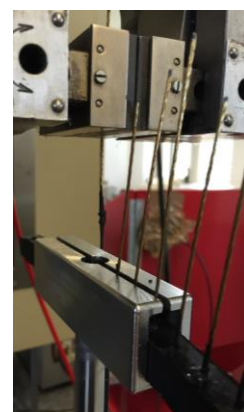


Figure 12- Standard T-Test Procedure

### 3.2.2 Peel Test

The specimen, in this case, is clamped directly on the tensile testing machine. Usually with steel cord, the specimen is characterized as two bonded layers of calendared steel cord. When the test starts the sample is opened, i.e. peeled, and the force required is directly measured by the testing machine. The value considered as the “peel force” is the median of all the values obtained throughout the sample while in the standard T-Test this is a single value, correspondent to the pull-out moment. The adhesion evaluation is made by measuring the force necessary to detach the two layers of steel cord (Peel Force) and by the rubber coverage shown in the cords. This last parameter is evaluated in a similar way to the standard T-test, differing on the scale: instead of 65 % to 100 %, it is evaluated from 1.5 to 5 with a 0.5 unit step.

## 3.3 Tests design and sample preparation

On the development of a test method, the test procedures along with the sample preparation are important, if not the most important, parts of the task.

As referred before, the carcass and the bead constitute the major load support system on the tire structure, helping to sustain inflation pressure, carrying the load, counteracting impact and coping with horizontal stress. This load on the carcass and its deformation, are changed rapidly while the vehicle is moving and the rubber-steel cord interface is affected by the number and extent of cycles. We can find in the literature that mechanical loading history, environmental effects and rubber formulation are the main factors for tire failure. Thus, it is crucial to develop a method able to reproduce these effects.

This section will be divided into the 3 different test methods, explaining all the steps involved until the final product is achieved.

### 3.3.1 Shear T-Test

This test focuses on simulating the cyclic loading of carcass in real service. The sample building is done accordingly with that fact, i.e., the rubber steel cord specimen was developed according to how they were adhered in a carcass. In summary, this is a 2-step method where the rubber/steel cord specimen is submitted to fatigue during a given number of cycles in the Frank Machine, assessing the adhesion a posteriori by standard T-Test in the Zwick Tensile Tester.

In a new test such as this one, investigations to discover the effects of different fatigue test parameters on the adhesion of rubber to steel cord should be carried out to find the correct and ideal parameter set to future studies.

*1<sup>st</sup> Investigation to discover optimal parameter setting*

The rubber compound used during these investigations was a standard compound used on Continental facilities. The steel cord used had the construction 1+ 5 X 0.4.

**Sample building**

The purpose was to build a sample similar to a standard T-Test sample. The main difference would be the number of cords and rubber rows. Usually, a standard t-test sample is characterized by a single row of rubber with 10 cords embedded, prepared and tested following these steps:

1. Place the 4 mm thick rubber compound on the back part of the mould;
2. Cut 10 cords with the correct length. Using one side of the mould((*Figure 13 a*)) - 10 cm; two sides-25 cm);
3. Put the cords on top;
4. Place the second layer of 4 mm thick rubber compound on the top part of the mould;
5. Pre-heat the mould with the temperature desired (150 °C - 170 °C) for, at least, 30 min;
6. Proceed to the sample curing, putting the samples in the pre-heated mould for a defined time (10 min - 30 min);
7. Remove the samples from the mould and wait, at least, 3 hours to proceed to testing.
8. If the samples need to be humidity aged, apply the anti-corrosive paint on the cords. If not, proceed to step 10;
9. After waiting one day to dry the samples, place them on the oven at 70°C for 14 days(Medium Humidity);
10. Test it following the Standard Static adhesion T-Test procedure, explained in section 3.2.1;

However, the samples intended to build are slightly different. They have two rows of rubber compound connected by 20 steel cords, instead of the single row with 10 cords. This brings the problem that there is no mould which could allow the sample building under these circumstances. Two options would remain: either design a new mould suitable to these specifications or find a solution with the current mould. Considering that the first option would take a considerable amount of time to start this test, which within this thesis timeframe was promptly ruled out, the second choice was preferred.

Thus, the solution found was to merge two identical moulds, putting them side by side during preparation and curing, modifying some preparation steps comparing to the standard sample (1, 2, 4 and 7).

The only difference would be to double the content of rubber compound and cords, originating a sample as shown in *Figure 13 b*).

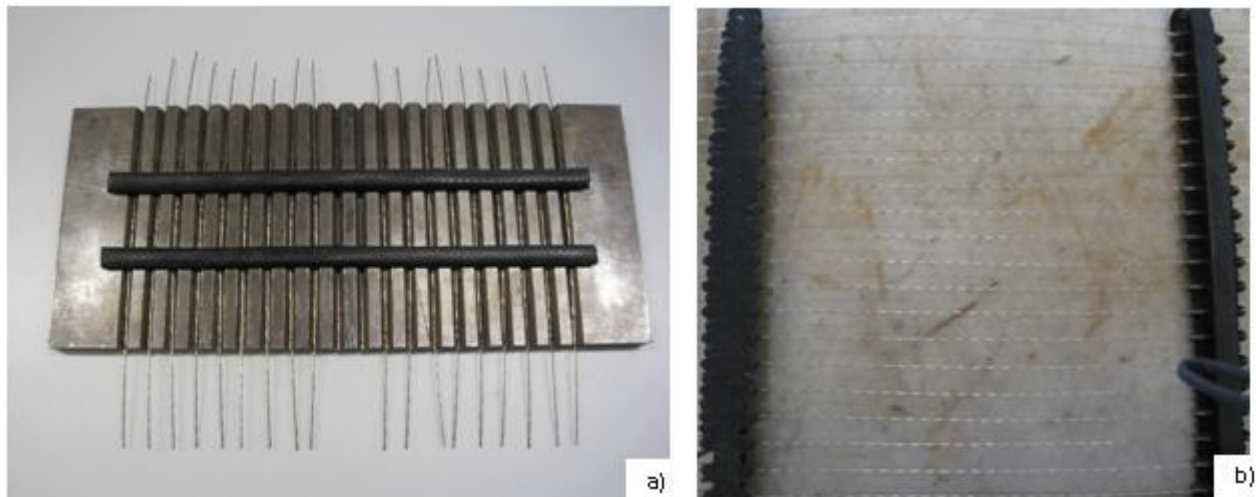


*Figure 13- Prepared samples a) 4 standard samples in the preparation mould b) Modified T-Test Sample.*

In this specific case, the samples were cured for 20 minutes at 160°C. 13 samples were built for this first investigation.

#### **Parameter setting**

The purpose for this investigation was find the correct set of fatigue parameters in which an effect on the steel cord-rubber adhesion layer after the fatigue could be seen.

As explained earlier, two different loadings can be applied on Frank Machine: tension or compression. Although there is a small hint that tension could be the correct fatigue mode, the experience will be conducted on both. 6 of the samples would carry the tension investigation and other 6 would be fatigued by compression. The thirteenth sample would be tested without fatigue, being considered as the 'reference' sample. Considering the limitations of the Frank Machine and the results obtained by the Chinese group of researchers, the first setting defined was the following:



*Table 1- Parameter setting 1<sup>st</sup> investigation.*

Parameter	Defined setting
Frequency/Hz	5
Amplitude ( P-P)/mm	4
Temperature/ °C	RT
Number of cycles	2x10 <sup>6</sup>

Before placing the samples on the Frank Machine, required adjustments on the machine should be done. All samples should be placed and clamped applying the same force. The two top and bottom cords should also be cut allowing the correct placement of the samples. After the sample placement, the machine ought to have a similar aspect to the presented in *Figure 14*.

*Figure 14- Samples placed on Frank Machine.*

It is also stated that, finished the fatigue, a period of 32 h should be respected before testing.

### Testing and observed behavior

After the finish of fatigue and the waiting period of 32 h, the 16 steel cords between the two rubber bars were cut into two equal lengths. Then, they should be tested using the Zwick Tensile tester, at a crosshead of 50 mm/min, according to ISO 5603:2011. Each of the bars is tested in two different measurements, where each measurement represents the average value of 16 cords.

Consider as the “reference” the value of a fresh/non-fatigued sample. The average of two “pull-out” force measurements was considered as the result evaluating also the rubber coverage of the samples:

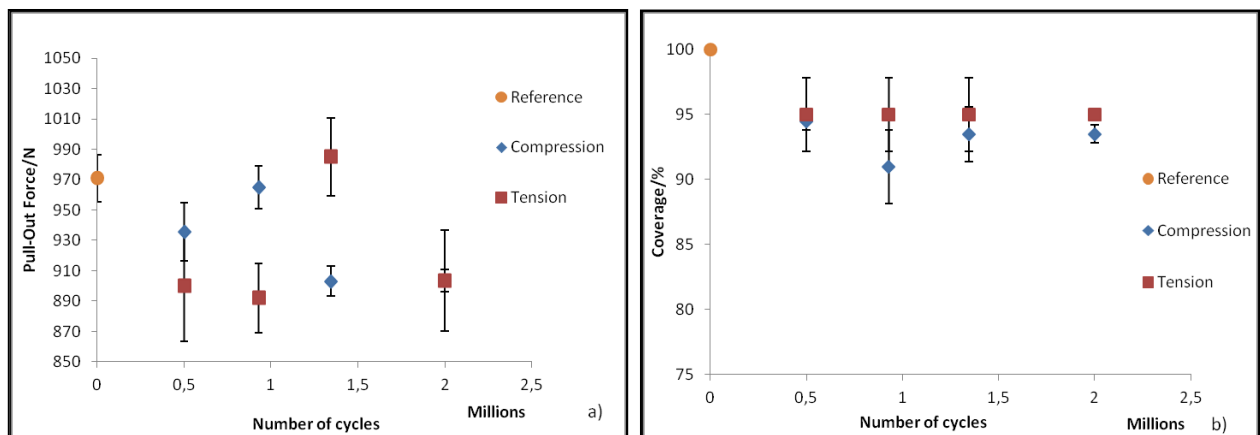


Figure 15- Influence of compression/tension in a) Pull-out force b) Coverage.

Observing the two graphs, it stands out an unpredictable behavior, with constant increases and decreases, mostly in the pull-out force. Nothing can be concluded from these data concerning the parameter setting, being absolute clear that no pattern is observed nor even which type of loading is more promising over the other. It would be important, then, to try to understand the causes that support these results and which causes could have been responsible. The first possible cause could have been the sample preparation: considering that it was the first sample setting prepared, some mispreparation and small errors during sample building may have happened and could have contributed to such results.

Then, two more samples were prepared and cut in different positions on the rubber bar. Some bubbles were visible on the top part of the samples, leaving the hint that the curing process was not effective. This could also be explained with the fact of the curing press in use was having some issues: the temperature at the center of the curing press was within the temperature range intended ( $\pm 0.5$  °C) but the rest of the press was out of bounds, having temperature offsets of 2 °C. This would not be a problem in the curing process of the standard samples since they only use the press center part. However, these samples are double of the size of the standard samples and part of the mould would be in this area where

the temperature is out of bounds. Summarizing, another approach would be necessary in order to achieve the right test set for this method.

## *2<sup>nd</sup> Investigation to discover optimal parameter setting*

### **Sample building**

Considering the results obtained on the last investigation, another approach would be necessary. The solution found was to carry a 2-step curing process: half of the sample would be cured during 20 minutes at 160 °C, while the other rubber bar (uncured bar) would be left outside of the curing press. When finished the curing of the first rubber bar, the same would apply to the second half of the sample. Once again, 13 samples were built.

### **Testing and observed behavior**

The parameter setting and the procedure followed were exactly the same as in the first investigation, except for the number of cycles. It was settled that one of the samples should be tested for a longer number of cycles, approximately 3.5 million. Once again, the average of two pull-out force measurements was considered as the result evaluating also the rubber coverage of the samples, obtaining the results described in *Figure 16* and *17*:

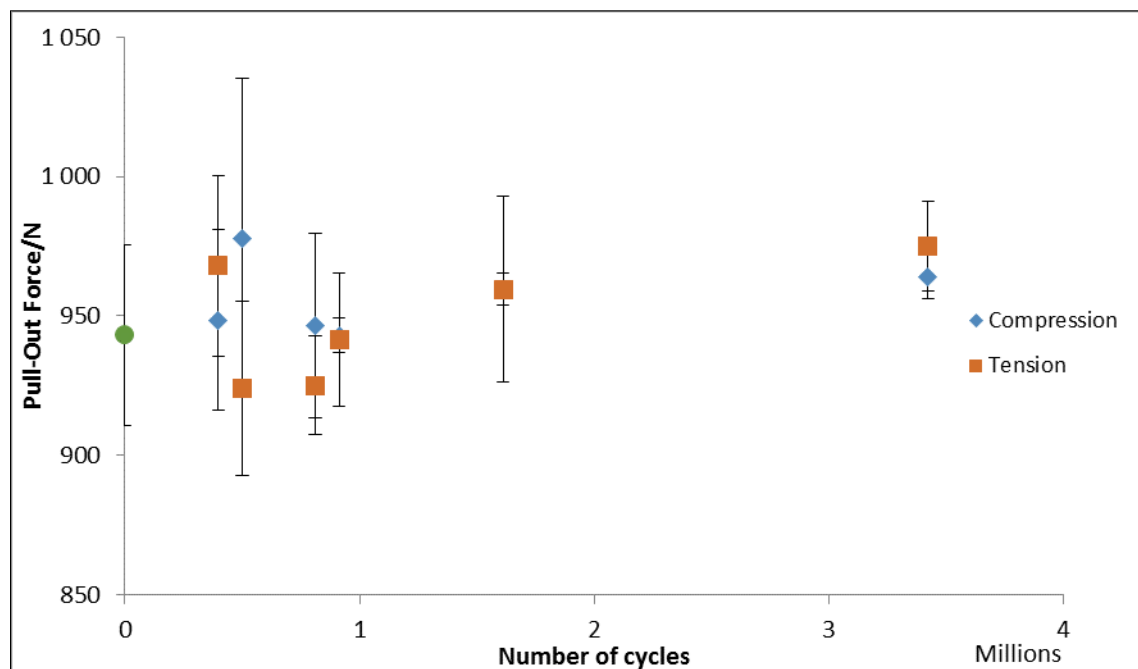


*Figure 16- Influence of compression/tension in POF on the 2<sup>nd</sup> investigation.*

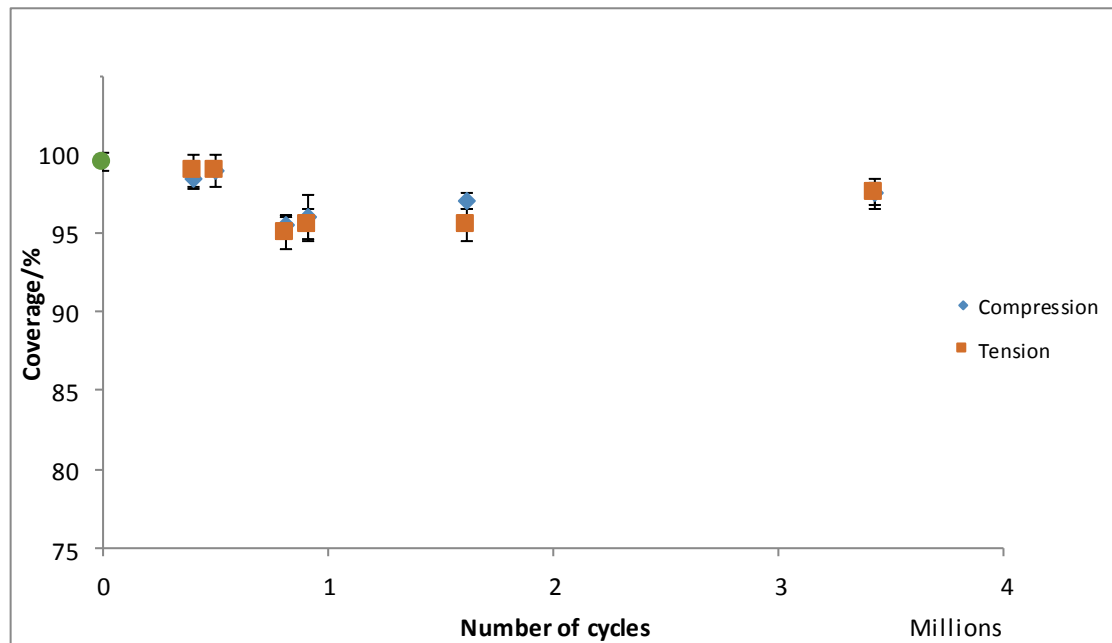
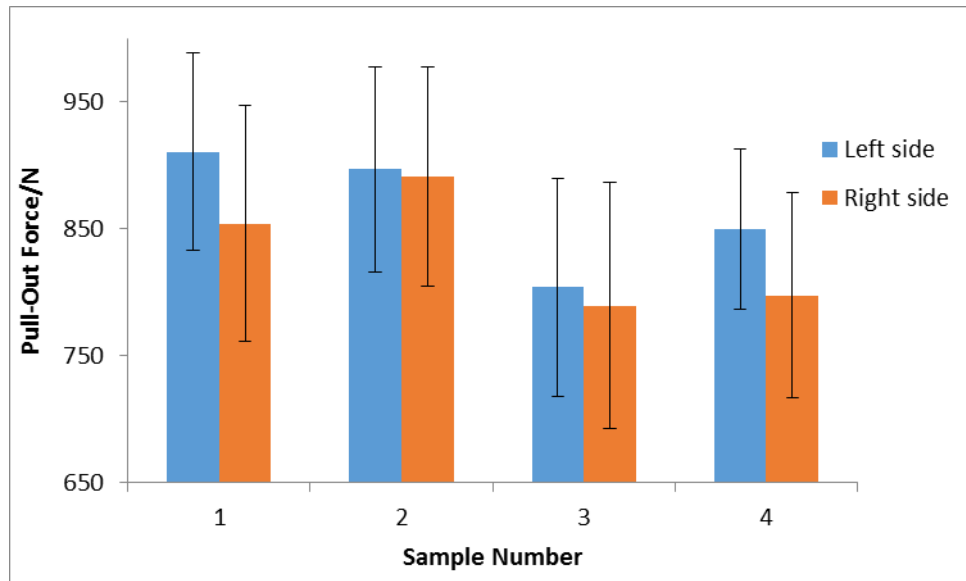


Figure 17- Influence of compression/tension in coverage on the 2<sup>nd</sup> investigation.

Analyzing first the POF graph, an erratic behavior stands out again, identically to the results achieved on the first investigation. Observing the coverage, no conclusions can be taken since the coverage is always close to 100%. This reveals almost null or even null effect on the adhesion layer after fatigue. Comparing to the results obtained in the first investigation, the average POF increased and the “bubbles” observed after curing were no longer evident.

Despite this fact, the results were irregular and the preparation or curing of the samples could be, once again, the only explanatory reason for this behavior. Furthermore, it is known that the POF value considered above is the average of 2 POF measurements, where which of them is also an average of 16 single cords POF values. Well, if the deviation within these 16 values is too high already, it becomes a difficult task to evaluate and obtain coherent results working with average values.

Thus, an evaluation on the spreading of the results inside the sample and sample by sample in the same conditions, i.e, the deviation between the 16 cords as well as the deviation between both rubber bars average, was carried out with 4 samples. All samples were fresh. That evaluation is represented on *Figure 18*.



*Figure 18-Test deviation evaluation.*

To allow a better comprehension of the figure, by left and right side it is intended to mean the two equal length rubber bars comprehending the average of the 16 single cord values. The error bars represent the standard deviation of the 16 single cord values obtained for each bar. In order to have confidence in the results, this evaluation should show that all the bars are on the same level with considerably small deviation values. However, the opposite was reflected, showing that the values gap between samples and even in each sample is too high to be able to take valid conclusions. This spreading of the results could have been caused by the constant pulling down of the cords during the curing process since half of the sample was always hanging on the outside of the curing press. Although this may not be the reason or, at least, the only explanation to cause these “irregular” results, it could have been the main factor to such data. In conclusion, another investigation should be carried out to find the correct parameter setting.

### *3<sup>rd</sup> Investigation to discover optimal parameter setting*

#### **Sample building**

The results obtained on the last investigation revealed a clear need that another approach would be required. This time, the purpose was trying to simplify the sample building. The idea, then, was to create the preparation/curing process as close to the standard sample preparation as possible given that it has been done for several years and its results are trustworthy. Since the mould (see *Figure 13 a)*) allows the preparation of 4 standard samples (corresponding to one modified T-test sample in size), it was settled to prepare two halves of the modified T-Test sample separately and then connect them with clamps, having a similar aspect to the *Figure 19*:



Figure 19-New modified T-test sample setup.

13 samples were built following the procedure explained in the section 3.3.1., with a curing time of 20 min and temperature of 160 °C.

#### Parameter setting

Once more, the purpose for this investigation was to find the correct set of parameters in which an effect on the steel cord-rubber adhesion layer after the fatigue could be seen. Given that it could be concluded from the coverage graphs that no effect was noticed on the adhesion layer, the older parameters could be short to visualize the desired effect. Then, the amplitude was increased to 20 mm. The point was to keep the Frank Machine with the same frequency as operated before but the machine noise as well as its instability with so high amplitude set the limit at 4.5 Hz. The experience was conducted again on both loading types (compression and tension). Due to time limitations, the number of cycles was shortened to 2.5 million. The setting defined is resumed on Table 2:

Table 2- 3<sup>rd</sup> Investigation Parameter settings.

Parameter	Defined setting
Frequency/ Hz	4.5
Amplitude ( P-P)/mm	20
Temperature/ °C	RT
Number of cycles	2.5 x 10 <sup>6</sup>

### Testing and behavior observed

The procedure was similar to the other investigations differing only after the fatigue, where instead of cutting the sample in two equal length steel cord rubber bars, it was just required to loose and remove the clamps.

The results are described on *Figures 20 and 21*:

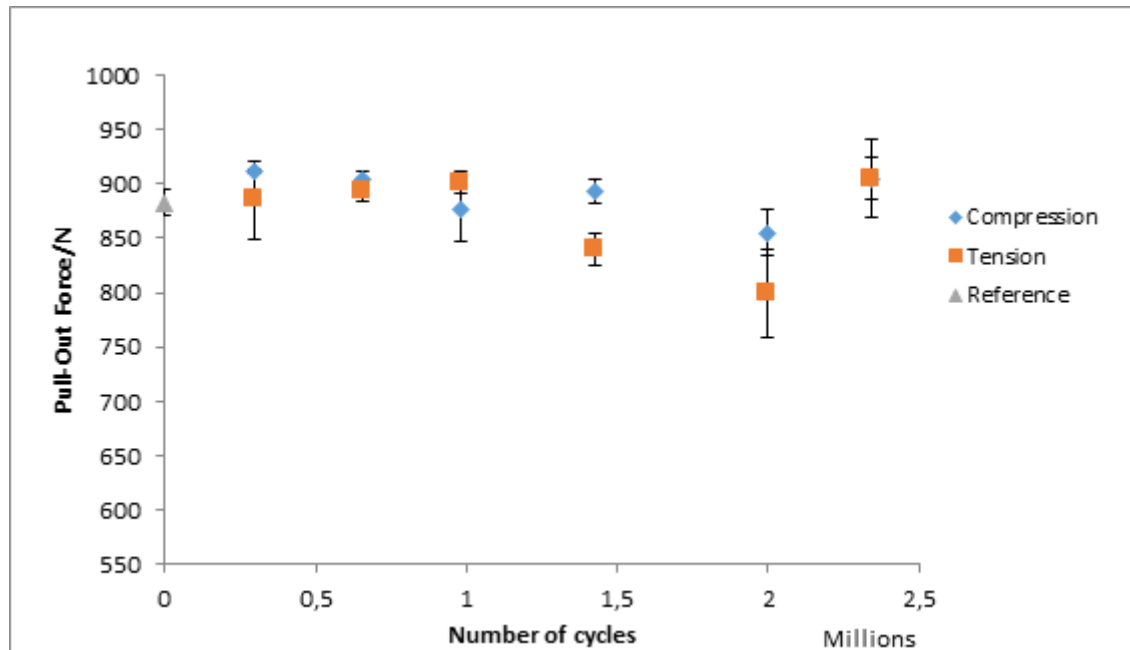


Figure 20- Influence of compression/tension in pull-out force.

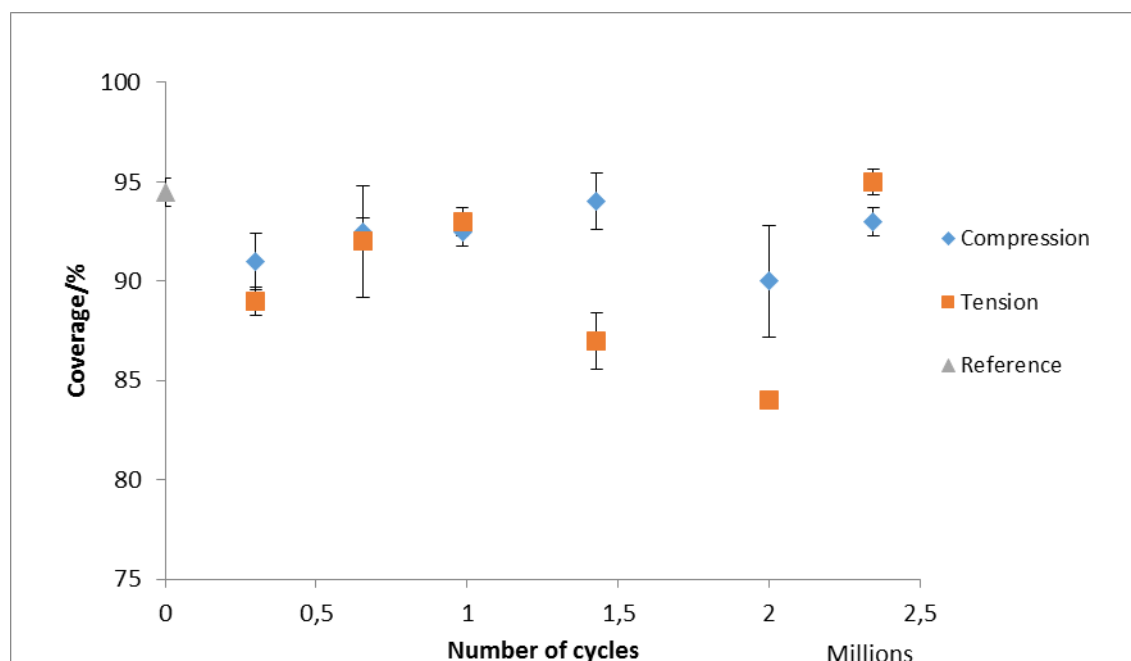


Figure 21- Influence of compression/tension in coverage.

Analyzing first the POF graph and recalling the older results, it is clear that the erratic behavior is finally overcome. The results in tension are now in line with the discoveries of the Chinese researchers, where the POF increases slightly during the first cycles, dropping after about 1 million cycles. This is the point where the mechanical effects eventually take place, suggesting that the site of failure is moving towards the interface as the number of cycles increases, reducing considerably the POF value compared to the reference. The last point represents an increase on the POF, which, in theory, does not make sense. This point could be an outlier where something along the preparation, curing or even fatigue may have happened to the sample to cause this result. These results, although, may be an indicator in which direction to proceed, pointing towards tension somewhere around 1.5 and 2 million cycles. Note that the behavior observed in compression, where the drop on the POF was not significant, is in line with the expectation.

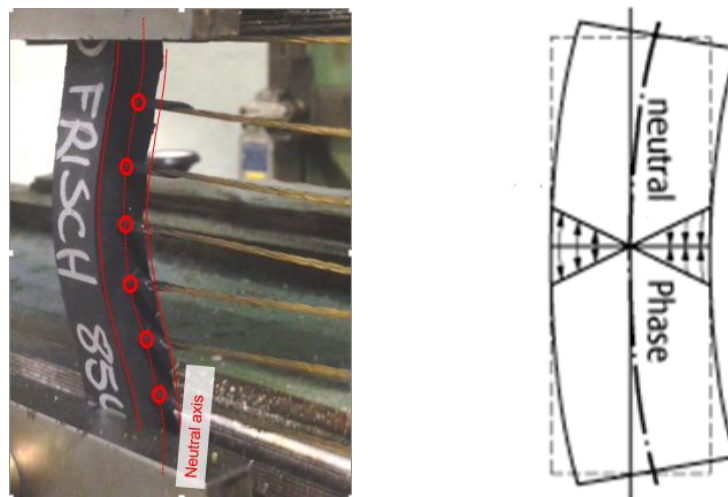
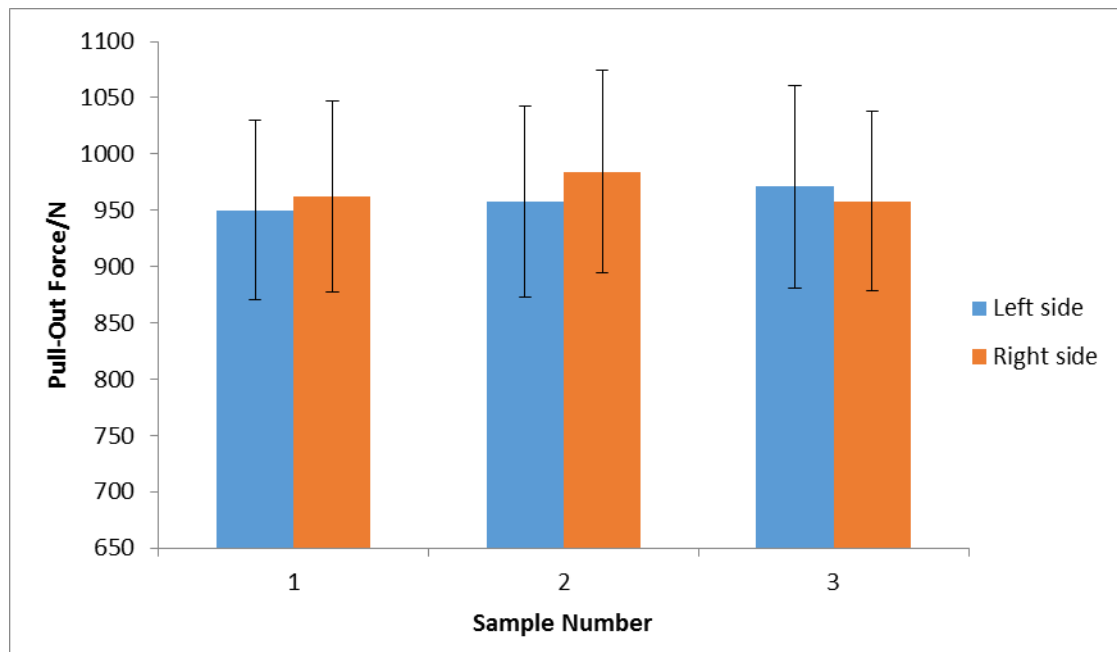


Figure 22- Samples in compression.

The expectation was that, by compressing the material, no shear forces were applied on the rubber-cord interface since the cord is at the center, in a neutral phase, as explained in Figure 22. At one of the sample margins the tension would be maximum while in the other the compression would be maximum. Anyway, at the center, in the rubber cord-interface, there is no force applied whatsoever, explaining why no effect under compression fatigue on the results was visible.

Thus, an assessment of the results spreading could be helpful to clear if the results are trustworthy. These results are shown in Figure 23. 3 samples were prepared and used for this purpose. Again, none of them are fatigued.





*Figure 23-Results spreading on 3<sup>rd</sup> investigation.*

As already mentioned, to rely on these results, this evaluation should show all the bars on the same level with considerably small deviation values. The deviation values are still high but all the bars are extremely close to each other, showing reproducibility on the results. This high deviation values is an intrinsic characteristic of the standard pull-out test, being absolutely normal this difference on the single POF values. Anyway, the last test set in tension was repeated in order to guarantee the reproducibility of the results.

Note that, in this repeated test, the compound used was taken from another batch, having the same recipe. The compound was the same but it belonged to a different production quarter. This “re-test” is shown in *Figure 24* along with the previous test.

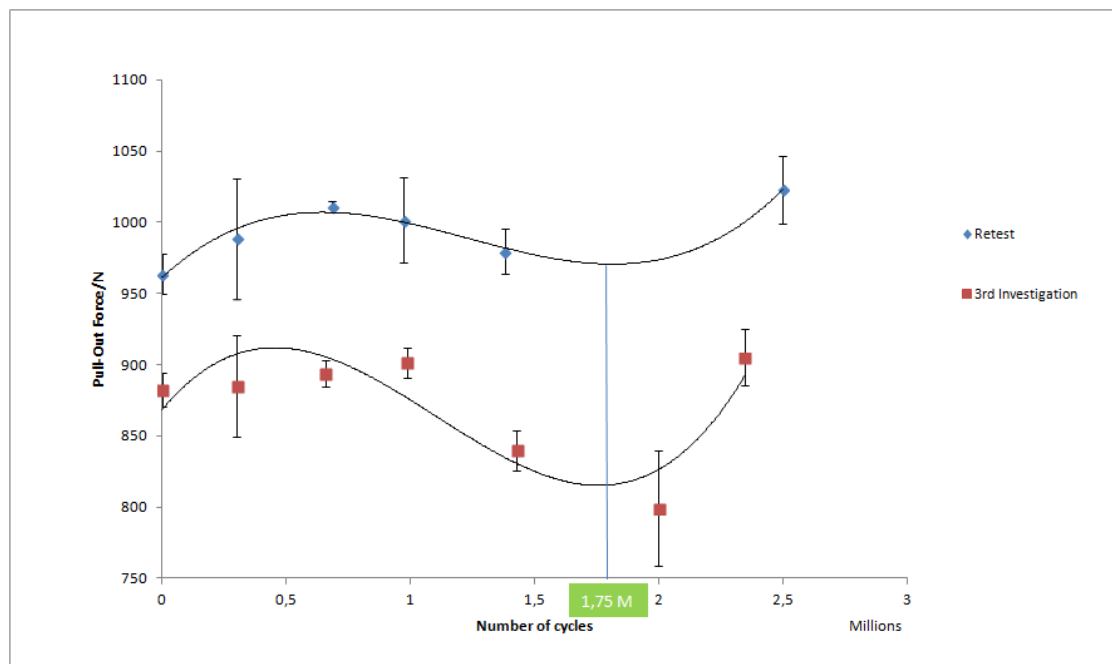


Figure 24- 3rd Investigation and re-test results in tension.

The previous results were pointing towards tension somewhere around 1.5 and 2 million cycles. The curve pattern visible on this “re-test” supported this assumption although with different absolute values. The increase at around 2 million happened once again. There is no feasible explanation for this effect.

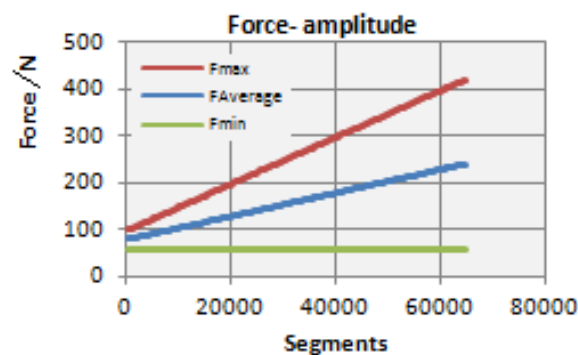
Nevertheless, there are two possible ways to analyze this result: taking into account the error bars, it is possible that all is equal and no effect on the adhesion layer is visible. However, considering that the goal was select a point where the adhesion layer would or could be affected, the best choice considering the results would be at 1.75 million. The sample building and the parameters are now set to test the 4 compounds and are listed below:

Table 3-Parameters set for Shear T-test.

Parameter	Defined setting
Frequency/ Hz	4.5
Amplitude ( P-P)/mm	20
Temperature/ °C	RT
Number of cycles	$1.75 \times 10^6$

### 3.3.2 Dynamic T-Test

This test is carried out on the MTS machine and comparing to the Shear T-Test, it reveals several advantages. First of all, it is characterized for being a one pass testing procedure, i.e, the dynamic conditioning and testing are on the same machine. The sample building is a well-known procedure, a standard T-test sample. The difference from the previous test is that the fatigue is done cord by cord which means that each cord is fatigued and pulled-out separately. The force level during the test is increasing with higher number of cycles, till the cord detaches the rubber, as shown in *Figure 25*. The static and dynamic load applied have a step of 1 N and 2 N , a range from 80 N to 500 N and from 40 N to 880 N, respectively. Each step is performed after 200 cycles.



*Figure 25- Increase of force level during test.*

Another advantage is the fact that this testing machine allows the variation of the temperature due to the existence of a temperature chamber which involves the testing device.

It not only allows the evaluation of the force applied during the dynamic procedure and consequently the maximum force at pull-out , but also the displacement on dynamic amplitude (two variables to assess the adhesion) and several other variables such as the dynamic stiffness and tangent  $\delta$ , as explained in section 3.3.2..

#### *Further parameters studied in the Dynamic T-Test*

Dynamic testing involves exciting a product or material sample with a controlled input and measuring the resulting response. A sinusoidal waveform input as a load or displacement signal is a common type of excitation imposed with a high performance servo-hydraulic actuator. The reaction load measured across the sample, the phase shift and the displacement signal are used to calculate engineering parameters, such as:

### 1. Complex dynamic stiffness, $K^*$

Vibration is merely a response to other conditions in a machine; it is not the fundamental concern of an engineer. Instead, vibration should be considered as the ratio of the forces acting on the machine to its stiffness, which is summarized by the equation:

$$\text{Dynamic stiffness} = \frac{\text{Force}}{\text{Observed Vibration}}$$

Since the dynamic stiffness is a vector, the complex dynamic stiffness itself is one orthogonal component of the dynamic stiffness. The component of the dynamic stiffness that acts in the same direction of the applied force is called the Direct Dynamic Stiffness, denoted by  $K_D$ . The component of Dynamic Stiffness orthogonal to this is known as Quadrature Dynamic Stiffness and is denoted as  $K_Q$ . When both Quadrature and Direct are included, it is generally referred to dynamic stiffness as Complex dynamic stiffness,  $K_{DS}$ . In Figure 26, the relationship between complex, direct and Quadrature dynamic stiffness is represented [20].

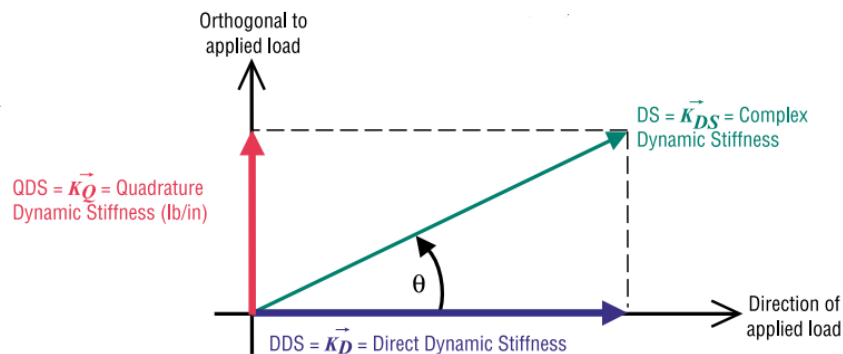


Figure 26- Relationship between complex, direct and Quadrature dynamic stiffness.

From now on, when referred to the complex dynamic stiffness, the notation  $K^*$  will be used to ease the process.

### 2. Tangent $\delta$ , $\tan \delta$

During dynamic material testing, the load and displacement data are used to calculate stress and strain cycles. The phase lag between the stress input and strain response is considered the  $\delta$ , as represented in Figure 27. It is also recorded and presented as  $\tan \delta$  or *loss tangent*.

This parameter is usually used to verify the effects of a given factor on the glass transition temperature of the rubber compound, by comparing the  $\tan \delta$  peak decrease to the reference conditions.

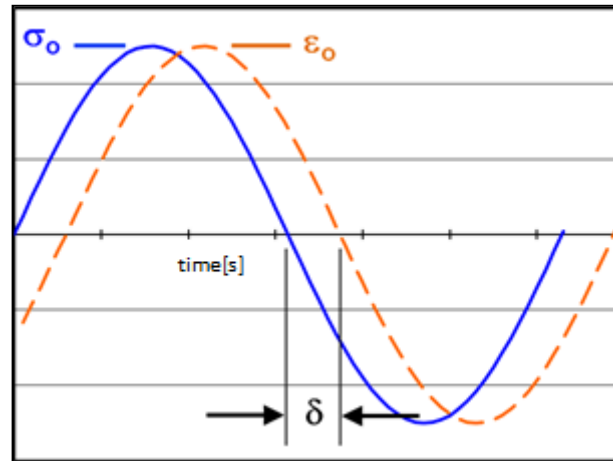


Figure 27-Phase lag between stress input and strain response [24].

#### Parameter setting

Similarly to what happened on the Shear T-Test, investigations on effects of different fatigue test parameters on the adhesion of rubber to steel cord were carried out to find the correct and ideal set for future studies. In this case, part of the investigations were prior to this research.

In the first prior investigation, the test ran for more than three million cycles at 20 Hz and room temperature, with no detection of weakening visible by observation of the  $\tan \delta$  which was kept constant. Another set of tests was defined, as listed in the table below:

Table 4- Defined parameters for testing.

Parameter	Test 1	Test 2	Test 3	Test 4	Test 5
Frequency/ Hz	5	10	20	20	30
Temperature/ °C	RT	RT	RT	80°C	RT
Number of max cycles	1x10 <sup>6</sup>	1x10 <sup>6</sup>	1x10 <sup>6</sup>	1x10 <sup>6</sup>	1x10 <sup>6</sup>

After performing the tests, the  $\tan \delta$  results were observed again. It is important, then, to point out that at 80°C, a clear weakening effect was observed, with a visible drop of more than 15% when compared to the other tests, as shown in Figure 28. The exact same effect in the POF is also observed, as shown in Figure 29.

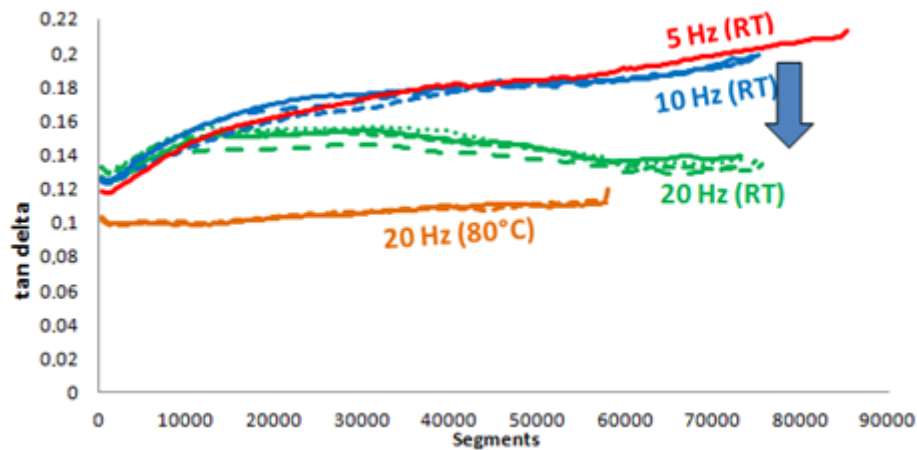


Figure 28-  $\tan \delta$  curves.

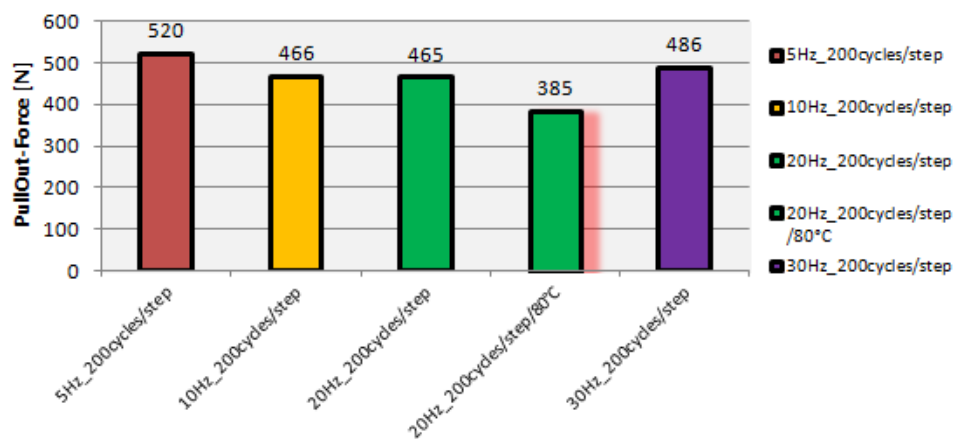


Figure 29- Pull-out force values.

The parameters were, then, defined to proceed with the testing:

Table 5-Defined parameters for Dynamic T-Test.

Parameter	Defined setting
Frequency/ Hz	20
Temperature/ °C	80 °C
Number of max cycles	Until pull-out

### Testing

The testing procedure should follow some basic rules to assure the reproducibility of the tests. The temperature chamber and the controller should be turned on before opening the MTS test software. The procedure explained in the **Appendix 1** should be followed.

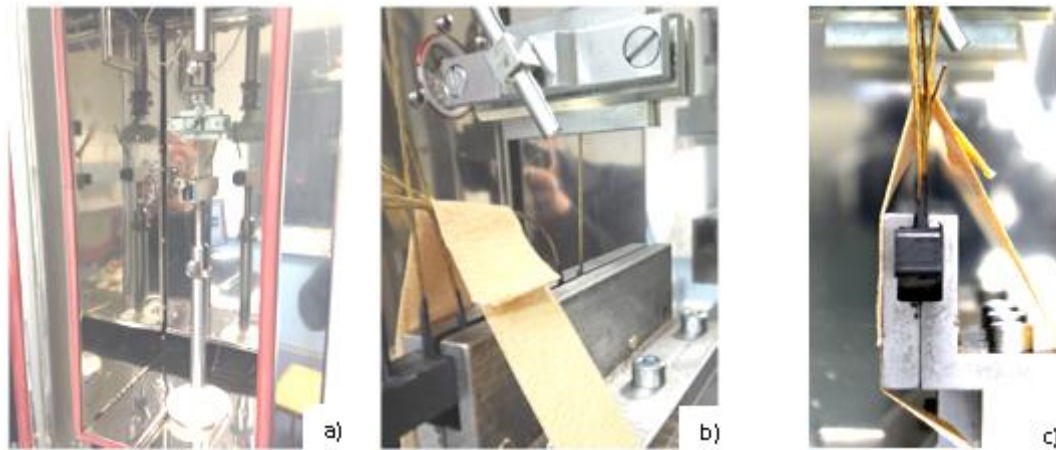


Figure 30-a) MTS Machine b) c) Samples set-up for testing.

The testing device along with the sample set-up for testing are shown in the Figure 30. When the cord detaches the rubber, i.e, the pull-out moment, the maximum force should be determined recurring to the following equation:

**Equation 1- Calculation of maximum force (pull-out Force)**

$$\text{maxforce} = \text{Static load applied} + \frac{\text{dynamic load applied}}{2}$$

Note that a cord should not be tested after a conditioning time superior to one hour given to the fact that the temperature eventually starts to damage the sample, affecting the results. Thus, the samples should be cut into sets of 2 cords.

### 3.3.3 3-Cord Adhesion

This test had, originally, the purpose to determine the static adhesion between steel cord and rubber. The objective is to include the dynamic variable on the system by fatigue on the Frank Machine in a similar way to the Shear T-Test, by bending the sample for a given number of cycles. The adhesion would be also assessed after the fatigue on the Zwick Tensile Tester, following a method similar to the Peel test. The sample building and testing procedure are described on the next sections.

#### *Sample building*

The material used was a serial standard rubber compound. Two layers of calendared steel cord (wound on a spool with equal spacing) with 26 cm length, 9.5 cm width and 1 cm thickness, are placed one over the other. 5 cm on the top of the sample should contain a small sheet of paper. In these 5 cm, sets of 3 cords should be separated with one cord of interval. These two steps will further allow the testing procedure. Then, the sample is placed

in the curing mould such as *Figure 30 a)*, cured for 30 minutes at 25 bar and 150°C, finalizing with the schematics similar to the *Figure 31 b)*.

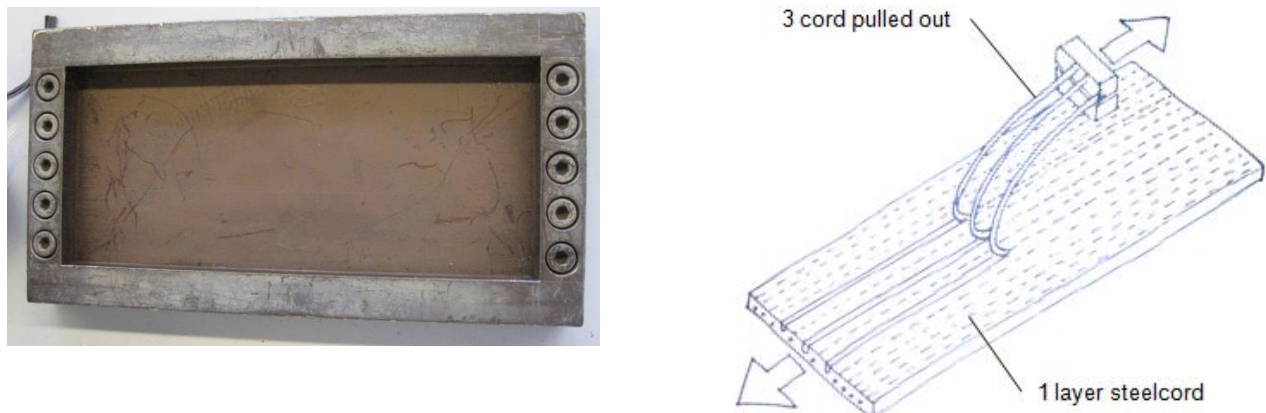


*Figure 31-a) Curing mould b) schematics of 3-cord sample.*

The original idea was to proceed with this sample set-up but after the vulcanization of the first sample, some irregularities on the steel cord were denoted. The solution found was to place one of the layers with a 22° angle comparing to the other, as shown in *Figure 32*.

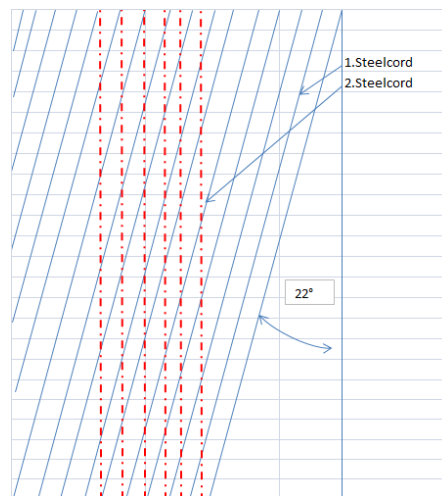


*Figure 32- New 3-cord sample building.*

These irregularities were eliminated with this new set-up, proceeding to further testing with the new set-up.

### Testing Procedure

After the sample curing, a waiting period of 3 h is recommended before testing. The cords bonded to the paper sheet should be removed. Then, place 3 cords at a time in the Zwick Tensile Tester with the set-up as the *Figure 33* shows. Before setting up the machine, zero the force. It is advisable to peel the first two or three cm manually to make sure the



material is conveniently clamped and everything is accordingly. Start the procedure on the Zwick software, recording the force curve, its mean value and evaluate the coverage from 1.5 to 5.



Figure 33- Zwick Machine Set-up for 3-Cord Adhesion Test.

#### *Parameters Setting*

In a similar way to the procedure followed on the Shear T-Test and Dynamic T-test, a prior investigation should be carried to done to find the correct fatigue parameters. The same parameter set as defined for the Shear T-Test is used as starting point. The parameters are listed on *Table 6*.

Table 6-Parameters setting for 3-Cord adhesion.

Parameter	Defined setting
Frequency/ Hz	4.5
Amplitude ( P-P)/mm	20
Temperature/ °C	RT
Number of cycles	$1.75 \times 10^6$

Two 3-cord samples were built. In each one of them, two sets of 3-cords were tested before fatigue in order to compare to the other two sets obtained after fatigue. If a decrease on the pull-out force or coverage was detected, it would mean that a weakening on the samples has occurred and that these settings could be used for further testing.

The results for this preliminary investigation are shown on the graphs, of *Figure 34* and *35*:



*Figure 34-Mean Peel-Force on Sample 1.*

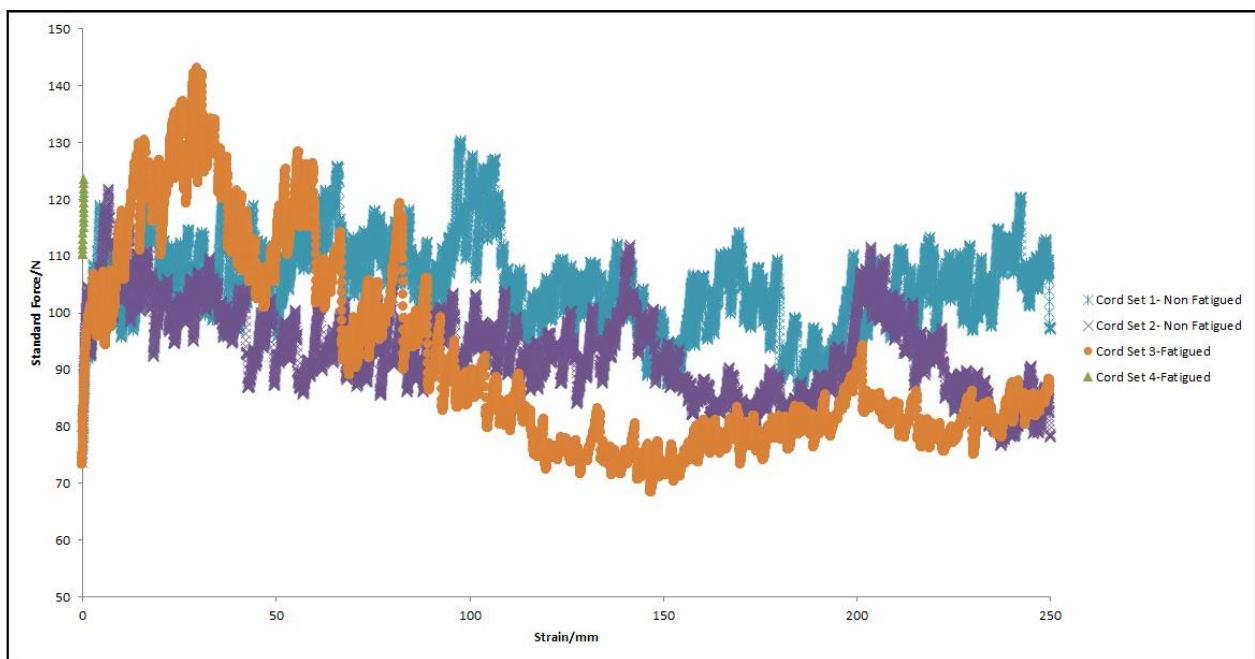


*Figure 35-Mean Peel-Force on Sample 2.*

By simple observation of both graphs, it can easily be concluded that no effect on the adhesion layer is visible due to the fact that none of the cords have shown a decrease of the peel force. In fact, in one of the cases the force required to separate the two layers is even greater after fatigue than in static conditions. Another parameter set is required. However, due to time limitations, this work is left for future studies.

## 4 Results and Test Method Validation

The idea was to elaborate a test that could allow us to test the dynamic adhesion of different compounds on a lab scale, defining a clear ranking between them. On the scope of this thesis, 4 different compounds will be tested (Reference + 3 experimental compounds). The reference compound is the compound used in CVT while the other three are “experimental compounds”, where the main difference resides on the substitution or reduction of the use of some environmental harmful chemicals.

Ideally, these test results will match the ones obtained with the built tire. In this chapter, the expected ranking will be disclosed and compared to the results obtained in the Shear T-Test and Dynamic T-test.

### 4.1 Expected results

In the plant, several tests were performed to analyze the performance of the four different tires given that the standard lab tests were showing no significant difference between them. These performance tests are drum-tests, in which it is simulated the service condition of the tire, calculating the number of hours until tire failure. Most of these tests were synchronized with the lab tests results, showing no difference between the different rubber compounds. However, one of them stands out showing a 50% drop on the rolling time, as shown in *Figure 36*:

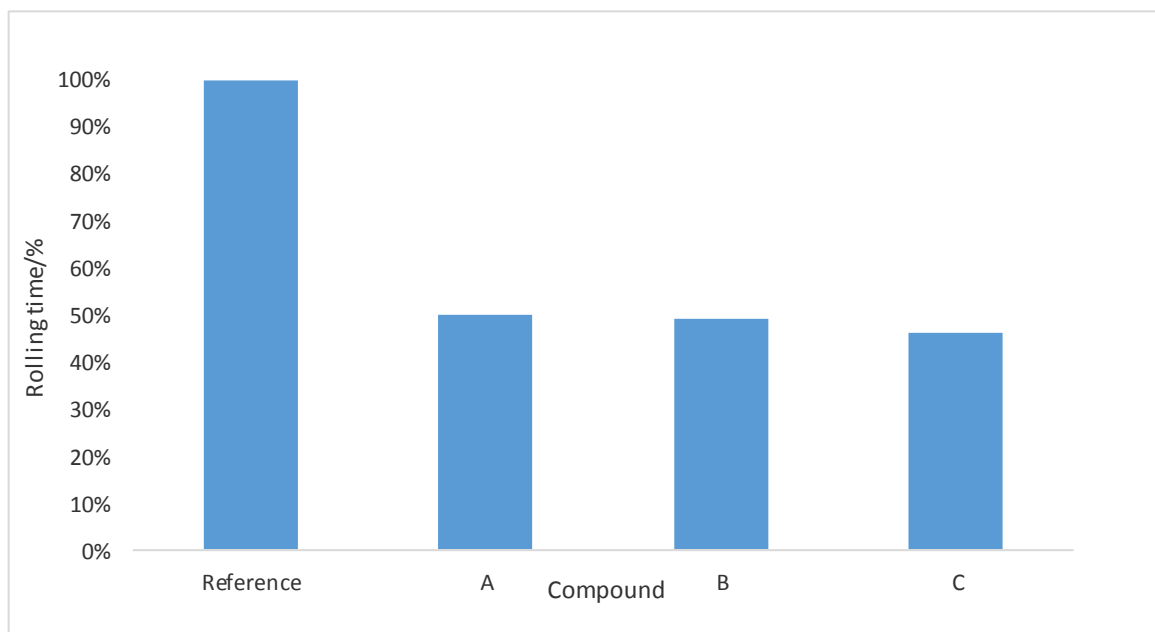


*Figure 36- Tire drum-test results.*

This test was held at extreme conditions, leading to tire failure. The results to obtain in the Shear T-test and Dynamic T-Test are supposed to follow this ranking in order to validate the test methods.

## 4.2 Test results

In this section, the results obtained in the Shear T-Test and Dynamic T-Test will be presented. Four different compounds were evaluated in two different conditions. It will also be evaluated the possibility to continue with these tests in the future. In the upcoming graphs, the following sample notation will be used:

*Table 7-Sample Notation.*

Sample	Notation
Reference Fresh	1
Compound A Fresh	2
Compound B Fresh	3
Compound C Fresh	4
Reference Humidity Aged	5
Compound A Humidity Aged	6
Compound B Humidity Aged	7
Compound C Humidity Aged	8

### 4.2.1 Shear T-Test

Two different ‘modified T-test samples’ were built for each of the 4 compounds. One of them was humidity aged while the other one was fresh, as listed on *Table 7*.

The parameters setting are accordingly to the *Table 3*, in section 3.3.1. The results are presented on *Figures 37* and *38*.

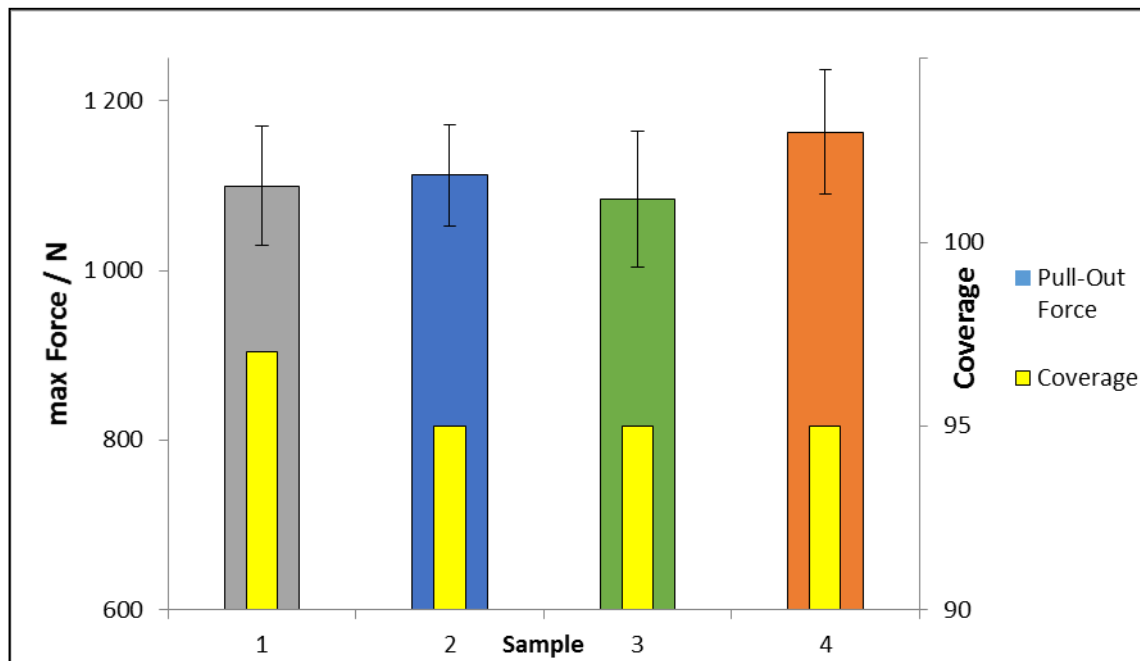


Figure 37- Results Shear T-Test in fresh conditions.

By observation of the Figure 37, it can be stated that no significant difference is observed between the four compounds pull-Out Force, being all the compounds really close to each other. As far as the coverage is concerned, a drop from the 3 experimental compounds is noted, in spite of not very significant.

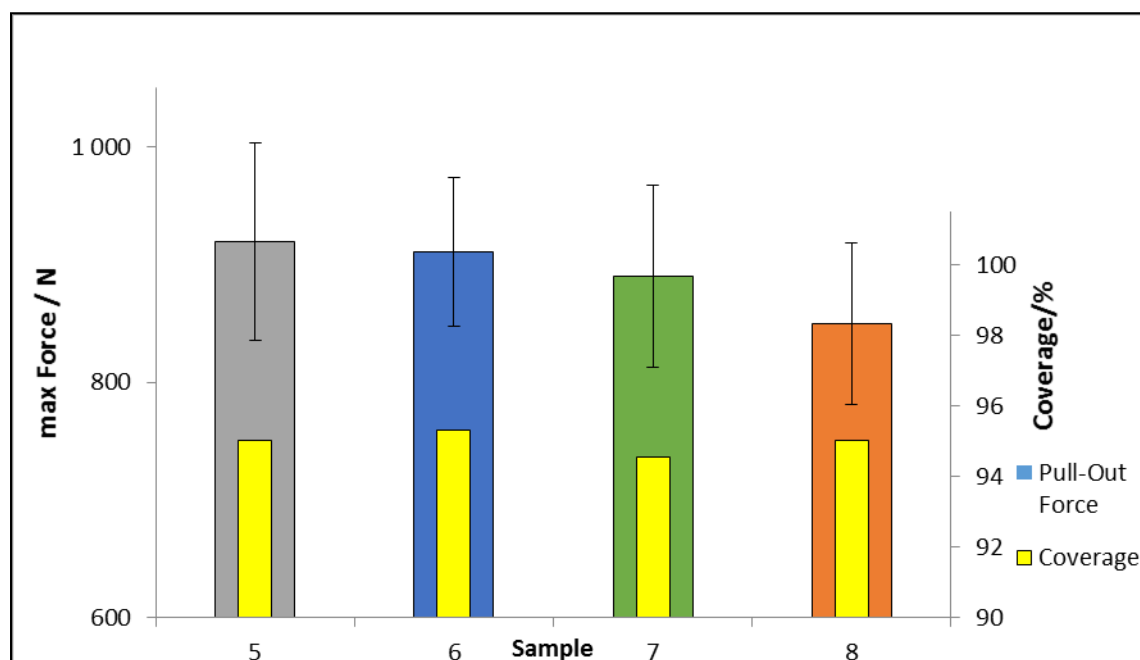


Figure 38-Results Shear T-Test under humidity aged conditions.

Under humidity conditions, a drop on the absolute value of the POF and at the coverage was expected. That fact was only verified with a 20% drop on the pull-out force.

The compounds ranking was still close to each other, denoting a small drop more visible on the compound C. As far as the validity of the test is concerned, this test did not reproduce the drum-test results. It is now clear that the non-inclusion of temperature variable on the Frank Machine is a clear limitation, making sense to question if it is reasonable to make further investigations with this test method. Concluding, this test method was not validated.

#### 4.2.2 Dynamic T-Test

Similarly to the previous test, two different ‘standard samples’ were built for each of the 4 compounds. The parameter setting is accordingly to *Table 5*, in section 3.3.2. In this case, not only the POF and coverage but also the complex dynamic stiffness, dynamic amplitude displacement and  $\tan \delta$  data are analyzed. Given that there are too many variables to represent graphically, some of the results are displayed on *Table 8*, finding all the graphs left to present on the *Appendix 2*.

*Table 8-  $\tan \delta$  and  $K^*$  values in fresh conditions.*

Sample	1	2	3	4
$\tan \delta / -$	0.103	0.112	0.107	0.111
Complex dynamic stiffness / $\text{N}\cdot\text{mm}^{-1}$	91.56	82.77	89.42	83.69

In fresh conditions and starting with the  $\tan \delta$  results’ spreading, each of the four samples is really close to the other, not being easy to distinguish them. Concerning the dynamic stiffness, although there is a drop on the compound A and C when compared to the reference, the absolute values of the compound B are similar to the reference compound.

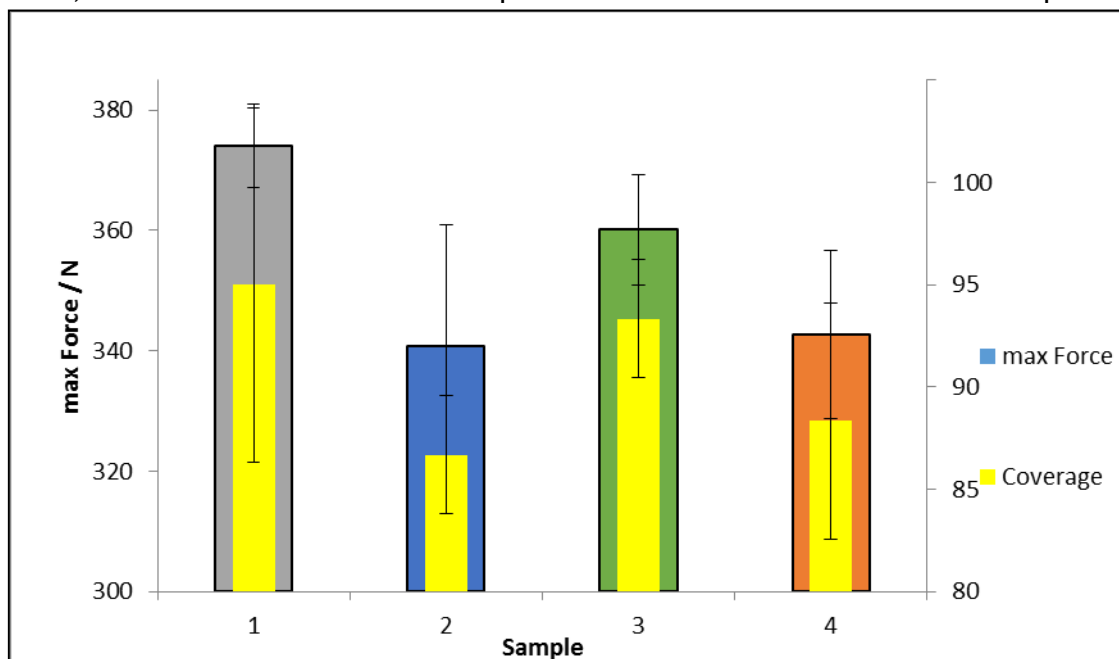


*Figure 39- POF and coverage in Fresh conditions.*

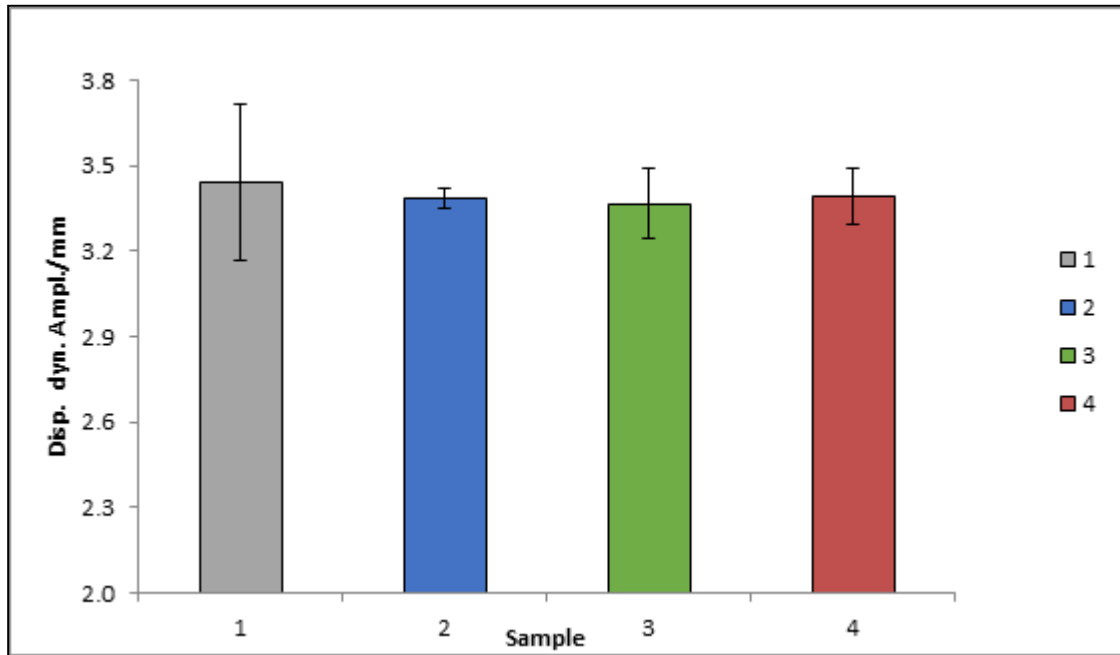


Figure 40- Dynamic amplitude displacement in Fresh conditions.

The same is applied to the coverage and pull-out Force (see Figure 39), and adding the fact that the variation observed on the dynamic displacement between the four samples is almost negligible (see Figure 40), it is reasonable to assume that these conditions do not reflect the expected results.

Regarding the samples under humidity aging conditions, some results are presented on Table 9:

Table 9-  $\tan \delta$  and  $K^*$  values in humidity aged conditions

Sample	5	6	7	8
$\tan \delta$ / -	0.105	0.108	0.108	0.110
Complex dynamic stiffness / $\text{N}\cdot\text{mm}^{-1}$	110.85	112.27	120.05	111.13

In a similar way to the results obtained in fresh conditions, both  $\tan \delta$  and complex dynamic stiffness were not helpful variables to successfully distinguish the four different compounds. The results of the pull-Out force and dynamic displacement were, however, a completely different scenario.

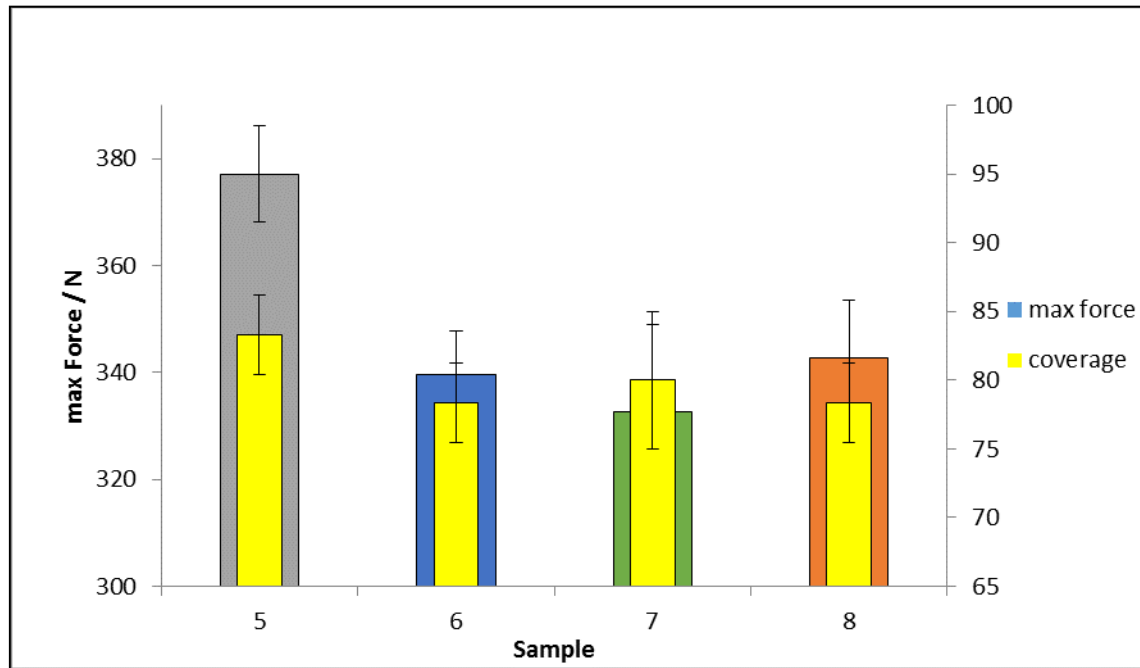


Figure 41- POF and coverage in humidity aging conditions.

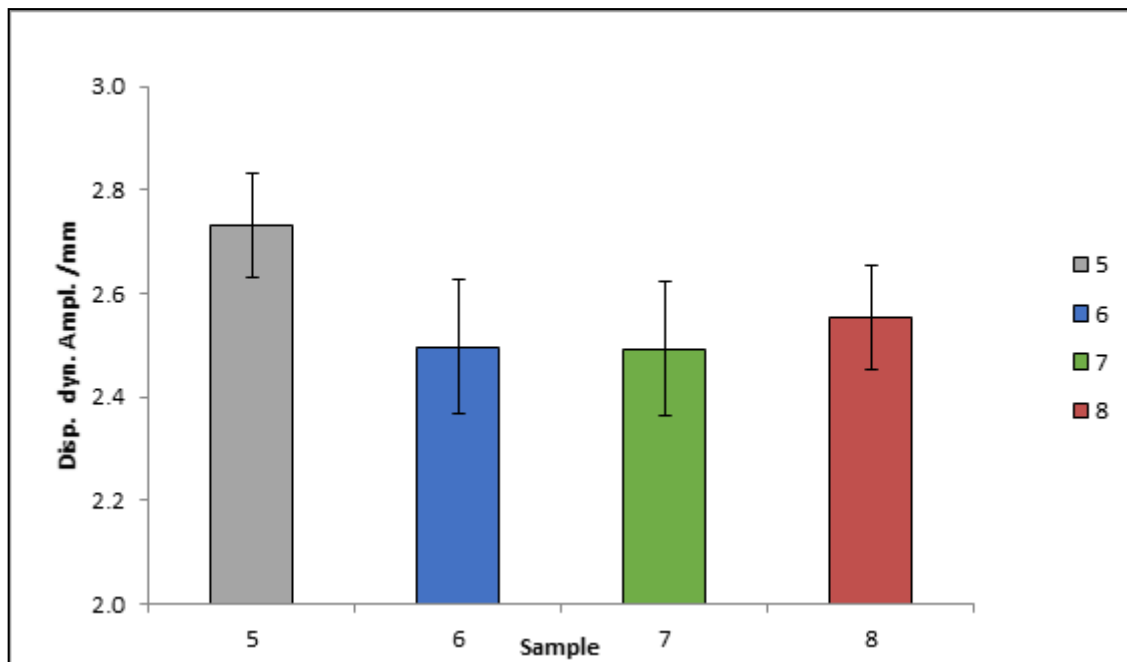


Figure 42- Dynamic amplitude displacement in humidity aging conditions.

By observation of Figure 41 and 42, it is clear the effect of the fatigue, observing a considerable drop not only on the pull-out force and coverage but also on the dynamic displacement amplitude in the three experimental compounds. These results match the tire test results, concluding that this test is promising and further testing can be done using this test method. This method is validated.



## 5 Conclusions

The goal of this project was to develop a test method capable to assess adhesion performance of steel cord to rubber in tire service conditions, i.e., under dynamic conditions. Two different tests were developed: shear T-Test and dynamic T-Test. A third test is under development. The results obtained from these tests should match with the results achieved in the tire drum-test to be considered as valid lab tests.

On the shear-T-test, parameters studies were carried out in order to find the most suitable set of parameters. These studies defined the loading type (tension), frequency and number of cycles. Finally, using ‘modified T-test samples’ in fresh and humidity aging conditions, the results did not match with the results obtained in the tire drum- test.

The dynamic T-test was also optimized. The best operating conditions are 80 °C on the testing device and 20 Hz on the hydraulic system. Using standard T-test samples, part of the results matched with the tire drum-tests under humidity aging conditions. With these results it was hypothesized that if the Shear T-Test was held in a device at a higher temperature, similar results could have been achieved.

The third test, 3-Cord Adhesion, is still in a preliminary stage of development. The sample building and the adhesion assessment test is completely defined. The parameter study failed to find suitable parameters for this test. Further investigation needs to be done in order to comprehend the capabilities of this test.

## 6 Project Assessment

### 6.1 Achieved goals

The development of a valid method capable to assess the adhesion between steel cord and rubber under dynamic conditions, reproducing the results on the tire drum-test as the final stage to validate the method was the main objective of this project.

At one of the tests (shear T-Test), the results were not satisfactory. However, the dynamic T-Test revealed itself as truly promising method for further testing. Under humidity aging conditions, the dynamic amplitude displacement and the pull-out force showed very similar behavior to the tire drum-test. This could represent the opportunity to analyze future compound recipes in adhesion performance without recurring to the drum-tests, leading to costs reduction and time saving, two of the most important factors at any industry.

### 6.2 Limitations and Future Work

Throughout the duration of this project, some limitations came along, most of them time related. In the Shear T-Test, new moulds appropriate to the intended sample could have been used but the time it would take to arrange it, within the time frame of this thesis, turned it into an impossible task. Furthermore, this test method could have more potential if the fatigue device allowed a temperature shift. About the 3-cord-adhesion test, further investigations should be performed in order to perceive the capabilities of this test.

### 6.3 Final Assessment

Since the first day, this thesis has revealed itself as a challenge: it is of great responsibility to create a test method since the roots, with no experience on the subject. It was sometimes difficult to know in which way to proceed, with the constant doubt if the choice made was the right one. Nevertheless, thanks to an always supportive team who was present the whole time whenever needed, a fair share of the goals was achieved. In a general way, the balance is very positive, with the certainty that everything was done to achieve the best results possible.

## References

- [1] Continental AG, "Facts and figures," [Online]. Available: [http://www.continental-corporation.com/www/portal\\_com\\_en/themes/continental/channel\\_facts\\_figures/facts.html](http://www.continental-corporation.com/www/portal_com_en/themes/continental/channel_facts_figures/facts.html). [Accessed October 2015].
- [2] Continental AG, "Tyre Basics Passenger Tires," [Online]. Available: [http://www.conti-online.com/generator/www/au/en/continental/tyres/general/downloads/download/reifengrundlagen\\_en.pdf](http://www.conti-online.com/generator/www/au/en/continental/tyres/general/downloads/download/reifengrundlagen_en.pdf). [Accessed October 2015].
- [3] K.Chandra e R. Mukhopdyay, "Studies of Dynamic Adhesion between Steel Cord and Rubber Using a New Testing Method," *Elsevier*, 1995.
- [4] National Highway Traffic Safety Administration, *The Pneumatic Tire*, 2006.
- [5] VERT, "Reinforcing materials," [Online]. Available: [https://www.tut.fi/ms/muo/vert/10\\_reinforcing\\_materials/index.htm](https://www.tut.fi/ms/muo/vert/10_reinforcing_materials/index.htm). [Accessed December 2015].
- [6] VERT, "Steel Cord Components," [Online]. Available: [https://www.tut.fi/ms/muo/vert/10\\_reinforcing\\_materials/index.htm](https://www.tut.fi/ms/muo/vert/10_reinforcing_materials/index.htm). [Accessed December 2015].
- [7] T. Kramer, "Basics of Reinforcements," in *TireAcademy*.
- [8] VERT, "Steel Cord Usage In Tyres," [Online]. Available: [https://www.tut.fi/ms/muo/vert/10\\_reinforcing\\_materials/index.htm](https://www.tut.fi/ms/muo/vert/10_reinforcing_materials/index.htm). [Acedido em Dezembro 2015].
- [9] W. Fulton, "Steel tire cord-rubber adhesion, including the contribution of cobalt," *Rubber Chem Technol*, 2005.
- [10] V. Ooij, "The role of XPS in the study and understanding of rubber-to-metal Bonding," *Surf Sci.*, 1997.
- [11] A. Coran, "The Science and technology of rubber," 2013.
- [12] W. V. Ooij, "Mechanism and theories of rubber adhesion steel tire cords-an-overview," *Rubber Chem Technology*, 1984.

- [13] B.Jurkowsi and J.Manuszak, "Dynamic Testing of Steel Cord/Rubber Adhesion," *Tire Technology International* 1995, 1995.
- [14] M. Jahmshidi, F.Afshar e B. Shamayeli, "Evaluation of Cord/ Rubber Adhesion by a new fatigue test method," *Journal of Applied Polymer Science*, 2006.
- [15] K.Mitsuhashi, "Methods of dynamic adhesion tests," *Nippon Gamu Kyokaishi*, 1981.
- [16] X.Shi, M.Man, C.Lia and D.Zhu, "Investigation on effects of dynamic fatigue frequency,," *Elsevier*, p. 9, 2013.
- [17] K.Mitsuhashi, "Dynamic adhesion fatigue tests II," *Nippon Gamu Kyokaishi*, 1981.
- [18] Zwick Roell, "Zwick Roell Website," [Online]. Available: <http://www.zwick.co.uk/en/products/static-materials-testing-machines/testing-machines-from-5-kn-to-250-kn/allround-line-materials-testing-machines.html>. [Accessed November 2015].
- [19] MTS, "MTS High-Force Servohydraulic Test Systems," [Online]. Available: [https://www.mts.com/ucm/groups/public/documents/library/dev\\_004848.pdf](https://www.mts.com/ucm/groups/public/documents/library/dev_004848.pdf). [Accessed November 2015].
- [20] S. Centerlines, "Understanding and Using Dynamic Stiffness," [Online]. Available: [http://www.ge-mcs.com/download/orbit-archives/1996-2000/2nd\\_quarter\\_2000/2q00tutorial.pdf](http://www.ge-mcs.com/download/orbit-archives/1996-2000/2nd_quarter_2000/2q00tutorial.pdf). [Accessed December 2015].
- [21] P. Patil, "Mechanism of improved aged rubber to brass adhesion using one component resins," *Rubber Chem Technology*, 2005.
- [22] P. Patil, "Mechanistic study of the effect of adhesion-promoter resins on the crystal structure of the copper sulfide adhesion layer at the rubber-brass interface," *Rubber Chem Technology*, 2006.
- [23] K. Rydberg, "Hydraulic servo systems," Linköpings Universit  t, 2008. [Online]. Available: [https://www.iei.liu.se/flumes/tmhp51/filearchive/coursematerial/1.105708/HydServoS ystems\\_part1.pdf](https://www.iei.liu.se/flumes/tmhp51/filearchive/coursematerial/1.105708/HydServoS ystems_part1.pdf). [Accessed December 2015].
- [24] "Continuum Mechanics," [Online]. Available: <http://www.continuummechanics.org/cm/dynamicmaterials.html>. [Accessed 2015 December].

## Appendix 1- Procedure Dynamic T-Test

The following procedure on the dynamic T-Test should be followed:

- 1) Heat the climatic chamber up to 80 °C, warming up at the same time the Hydraulic system in the Function Generator with a mean Level of 20 mm, Amplitude +/- 10 mm and frequency of 1 Hz;
- 2) Insert the sample as shown in *Figure 30 b)* and *c)* and allow a 30min conditioning, restarting the Function Generator;
- 3) Set the displacement to 0 mm, clamp the sample and close the chamber;
- 4) Proceed to the manual set-point of the Axial Force to 5 N until 80 °C are reached again;
- 5) Select the procedure: `Dynamischer_T-Test_Laststeigerung_stat80-500N_ohneBereichswechsel_II.000`;
- 6) Name it like that: `Order_Agingstatus_samplenummer_cord#1_20Hz_80°C_200cyc(date_time)`;
- 7) Start the Procedure (do not zero the Force (5 N));
- 8) Wait for the moment of pull-out (around 35 minutes), calculate the maximum force, collecting the values of the dynamic displacement, complex dynamic stiffness and the  $\tan \delta$  curve;
- 9) Calculate the maximum force;
- 10) Repeat the procedure for at least two more cords;

## Appendix 2- Graphs Dynamic T-Test

All  $\tan \delta$  as well as complex dynamic stiffness curves are represented on the figures below:

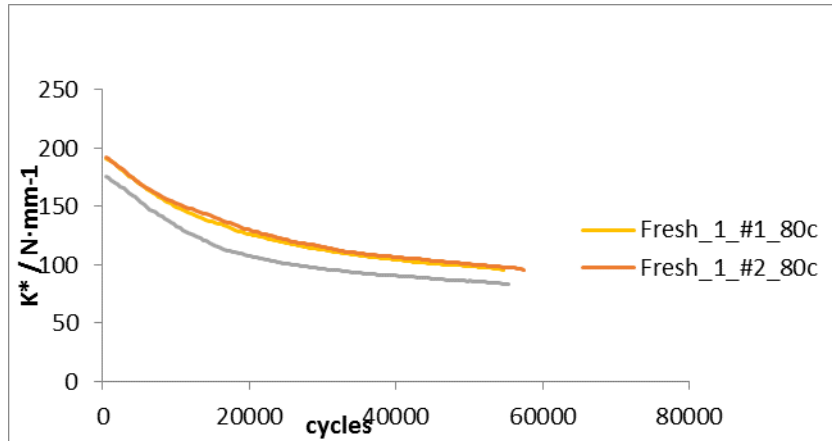


Figure 43- Complex dynamic stiffness curve in sample 1.

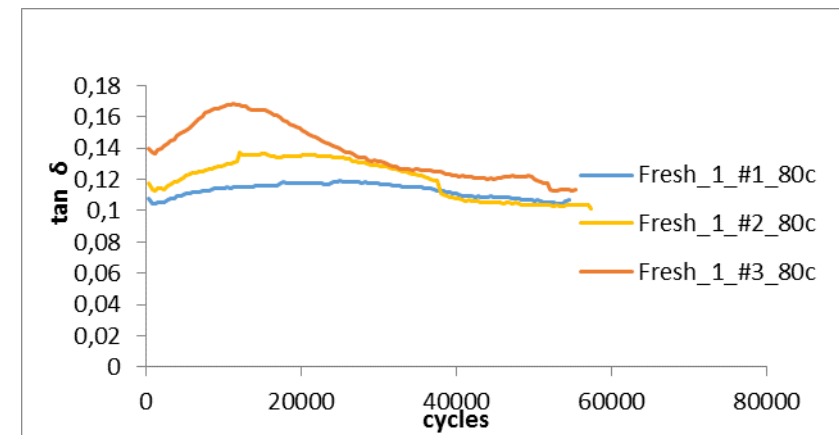


Figure 44-  $\tan \delta$  curve in sample 1.

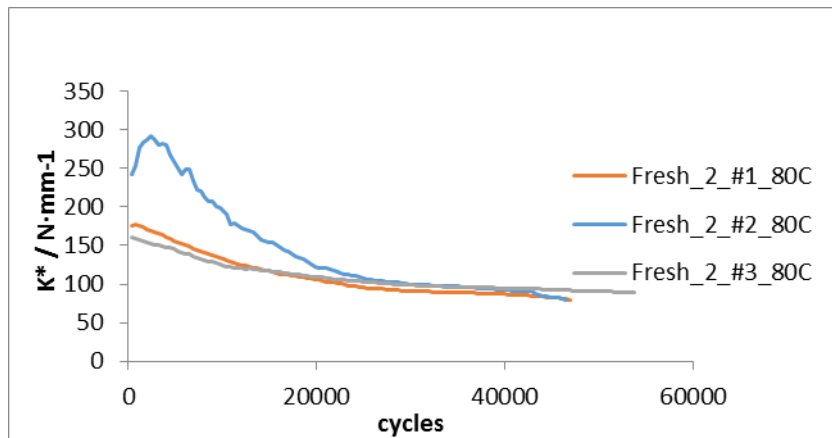


Figure 45- Complex dynamic stiffness curve in sample 2.

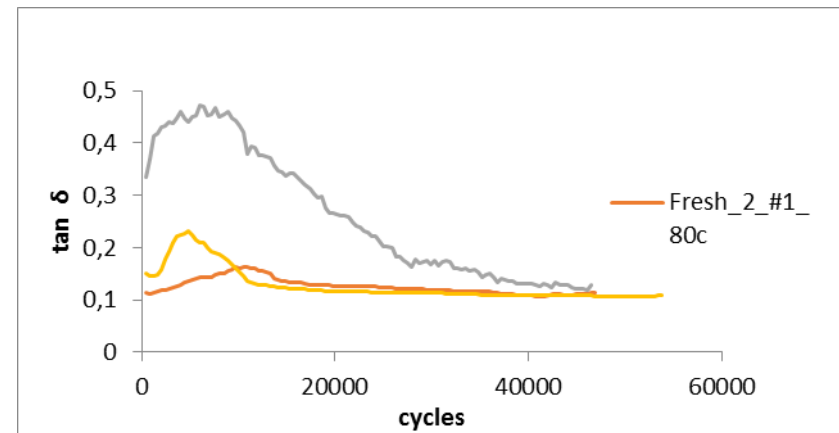


Figure 46-  $\tan \delta$  curve in sample 2.

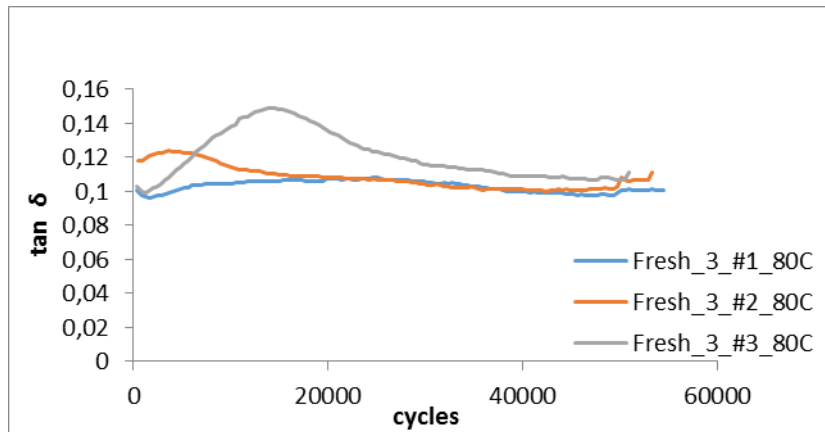


Figure 47-  $\tan \delta$  curve in sample 3.

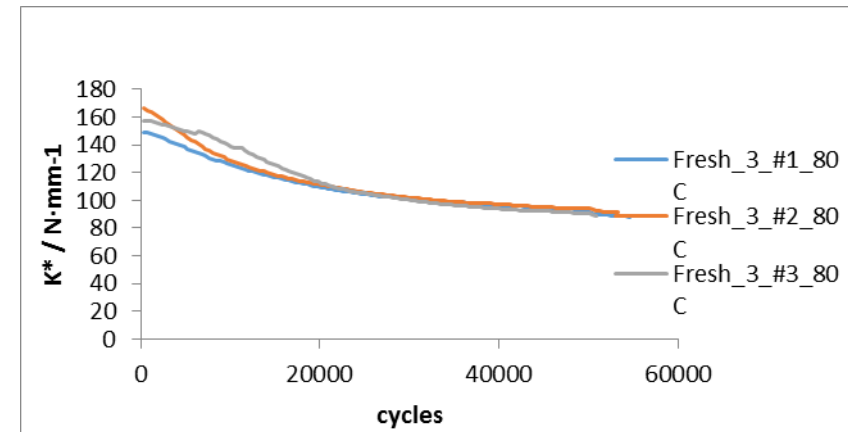


Figure 48- Complex dynamic stiffness curve in sample 3.

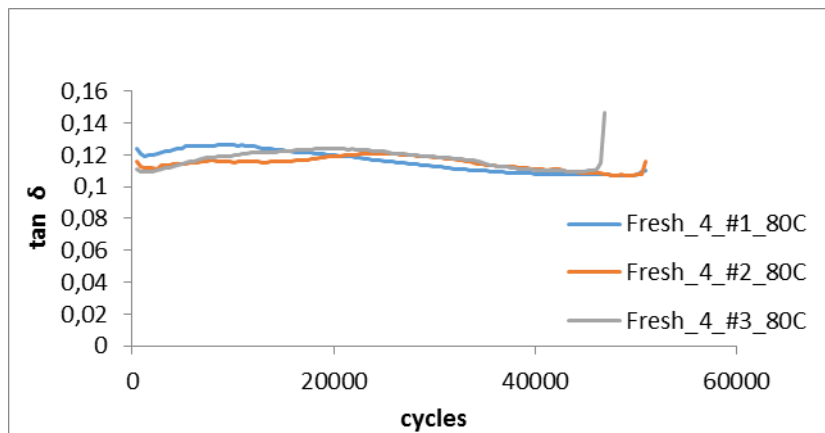


Figure 49-  $\tan \delta$  curve in sample 4.

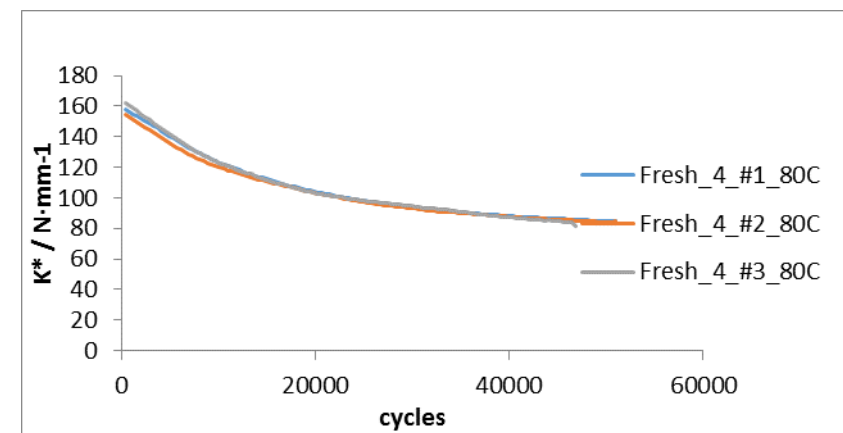


Figure 50- Complex dynamic stiffness curve in sample 4.

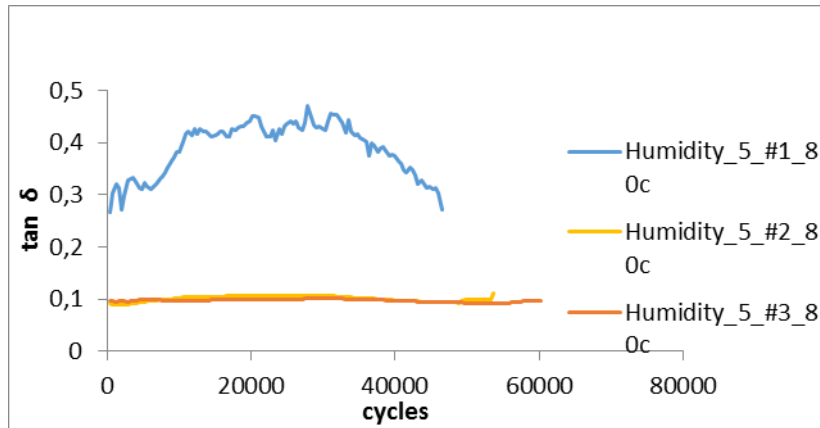


Figure 51-  $\tan \delta$  curve in sample 5.

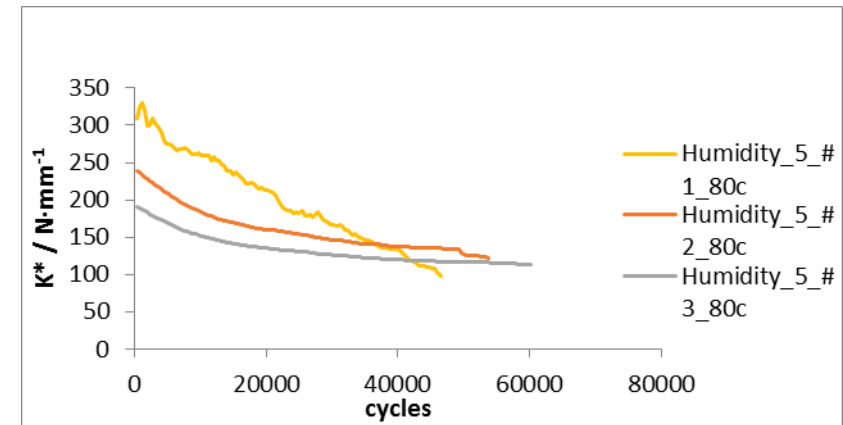


Figure 52- Complex dynamic stiffness curve in sample 5.

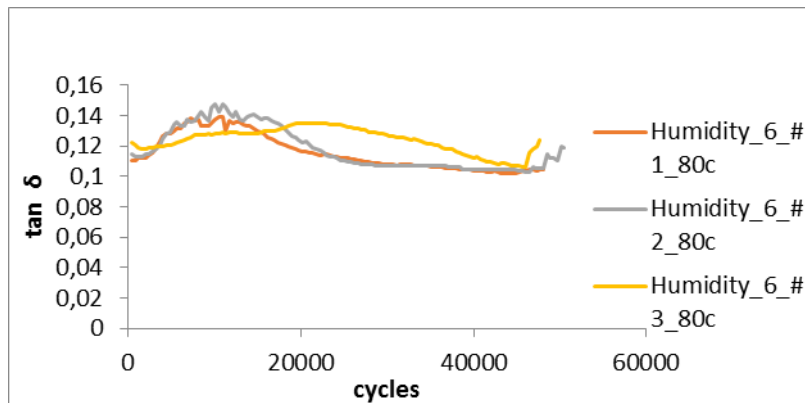


Figure 53-  $\tan \delta$  curve in sample 6.

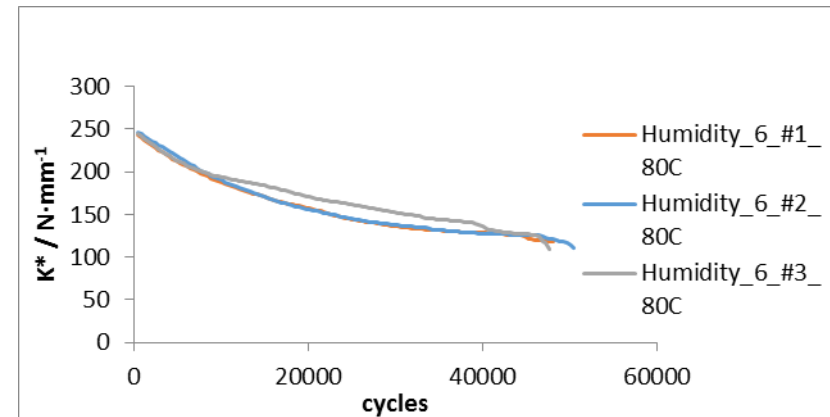


Figure 54- Complex dynamic stiffness curve in sample 6.



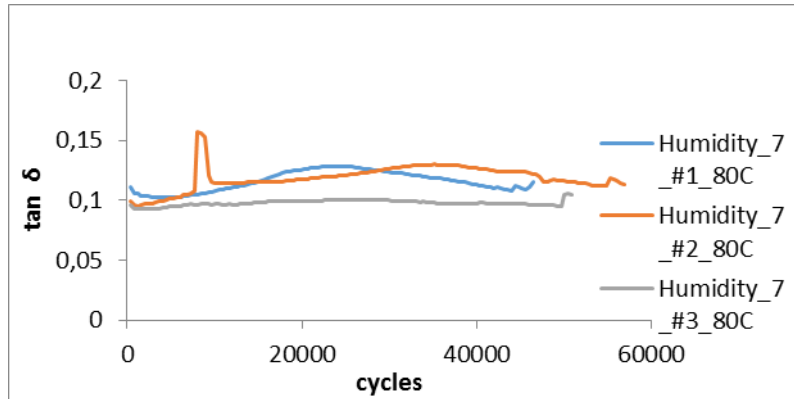


Figure 55-  $\tan \delta$  curve in sample 7.

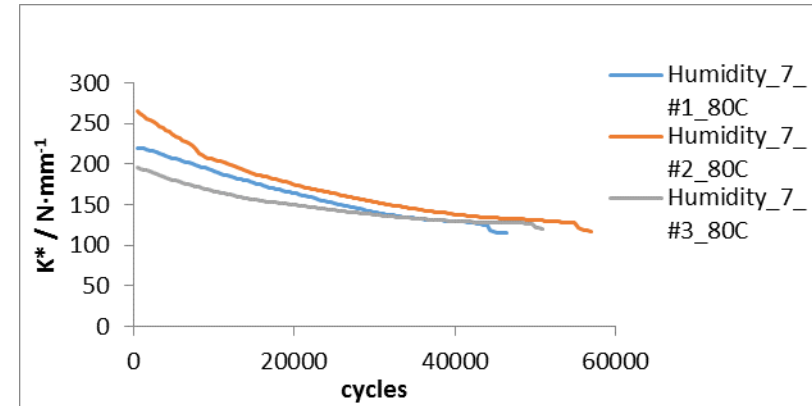


Figure 56- Complex dynamic stiffness curve in sample 7.

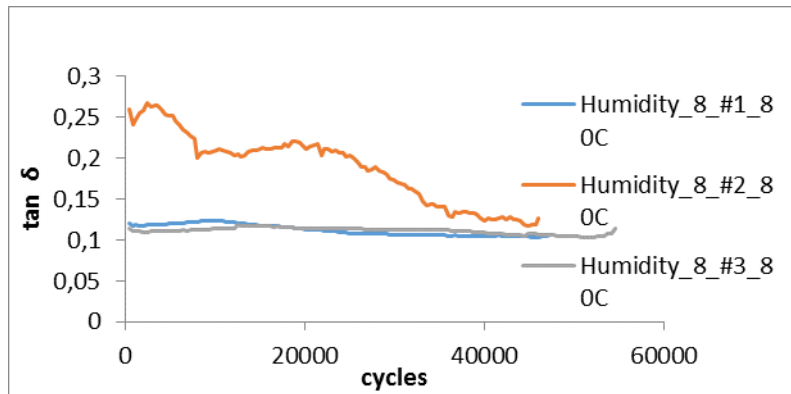


Figure 57-  $\tan \delta$  curve in sample 8.

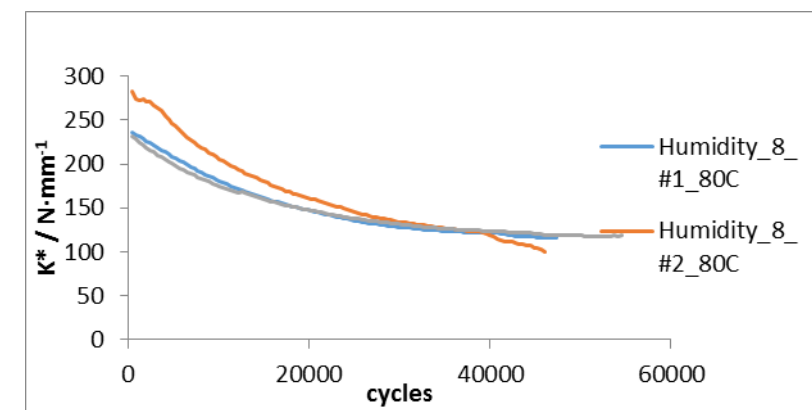


Figure 58- Complex dynamic stiffness curve in sample 8.